An oral inoculation infant rabbit model for *Shigella* infection

Carole J. Kuehl[*1,2], Jonathan D. D'Gama[*1,2], Alyson R. Warr[1,2], and Matthew K. Waldor[1,2,3#]

1.Division of Infectious Diseases, Brigham & Women's Hospital, Boston MA, 02115

2. Department of Microbiology, Harvard Medical School, Boston, MA, 02115

3. Howard Hughes Medical Institute, Boston, MA 02115

* equal contribution

for correspondence: mwaldor@research.bwh.harvard.edu

Running title (54 characters max): Oral inoculation model of shigellosis

Abstract (250 words max)

Shigella species cause diarrheal disease globally. Shigellosis is typically characterized by bloody stools and colitis with mucosal damage and is the leading bacterial cause of diarrheal death worldwide. Following oral ingestion, the pathogen invades and replicates within the colonic epithelium through mechanisms that rely on its type III secretion system (T3SS). Currently, oral infection-based small animal models to study the pathogenesis of shigellosis are lacking. Here, we found that oro-gastric inoculation of infant rabbits with *S. flexneri* resulted in diarrhea and colonic pathology resembling that found in human shigellosis. Fasting animals prior to *S. flexneri* inoculation increased the frequency of disease. The pathogen colonized the colon, where both luminal and intraepithelial foci were observed. The intraepithelial foci likely arise through *S. flexneri* spreading from cell-to-cell. Robust *S. flexneri* intestinal colonization, invasion of the colonic epithelium, and epithelial sloughing all required the T3SS as well as IcsA, a factor required for bacterial spreading and adhesion in vitro. Expression of the proinflammatory chemokine IL-8, detected with in situ mRNA labeling, was higher in animals infected with wild-type *S. flexneri* versus mutant strains deficient in *icsA* or T3SS, suggesting that epithelial invasion promotes expression of this chemokine. Collectively, our findings suggest that oral infection of infant rabbits offers a useful experimental model for studies of the pathogenesis of shigellosis and for testing of new therapeutics.

36 **Importance (150 words max)**

37 *Shigella* species are the leading bacterial cause of diarrheal death globally. The pathogen
38 causes bacillary dysentery, a bloody diarrheal disease characterized by damage to the colonic
39 mucosa and is usually spread through the fecal-oral route. Small animal models of shigellosis
40 that rely on the oral route of infection are lacking. Here, we found that oro-gastric inoculation
41 of infant rabbits with *S. flexneri* led to a diarrheal disease and colonic pathology reminiscent of
42 human shigellosis. Diarrhea, intestinal colonization and pathology in this model were
43 dependent on the *S. flexneri* type III secretion system and IcsA, canonical *Shigella* virulence
44 factors. Thus, oral infection of infant rabbits offers a feasible model to study the pathogenesis
45 of shigellosis and to develop and test new therapeutics.

Introduction

Shigella species are Gram-negative, rod-shaped bacteria that cause bacillary dysentery, a severe and often bloody diarrheal disease characterized by inflammatory colitis that can be life-threatening (1). This enteric pathogen, which is spread by the fecal-oral route between humans, does not have an animal reservoir or vector (1). Annually, *Shigella* infections cause tens of millions of diarrhea cases and ~200,000 deaths (2, 3). It is likely the leading cause of diarrheal mortality worldwide in individuals older than 5 years (2, 3). Most *Shigella* infections are attributable to *S. flexneri*, one of the four *Shigella* species, although in developed nations the prevalence of *S. sonnei* is higher (4–7).

The pathogen primarily causes colonic pathology that usually includes mucosal ulceration and erosion due to sloughing of epithelial cells, and is typically characterized by acute inflammation, with recruitment of neutrophils and plasma cells, congestion of blood vessels, distorted crypt architecture, and hemorrhage (8, 9). While inflammatory responses to *Shigella* invasion of colonic epithelial cells were thought to be the underlying cause of epithelial cell destruction and hemorrhage, recent evidence suggests that pathogen-mediated destruction of epithelial cells also plays a role in the development of pathology (10).

Shigella pathogenesis is attributable to a multifaceted set of virulence factors that enable the pathogen to invade and proliferate within the cytoplasm of colonic epithelial cells and evade host immune responses. The pathogen can also infect and rapidly kill macrophages (11). Most known virulence factors are encoded on a large (>200 kbp) virulence plasmid, which is required for *Shigella* pathogenicity (12–14). Key virulence determinants include a type III secretion system (T3SS) and its suite of protein effectors that are injected into host cells (15),

and the cell surface protein IcsA, which directs polymerization of host actin and enables intracellular movement (16, 17). The force generated by intracellular actin-based motility allows the pathogen to form membrane protrusions into neighboring uninfected cells, which the pathogen subsequently enters. Cell-to-cell spread is thought to promote pathogen proliferation in the intestine and evasion of immune cells (11). The ~30 T3SS effector proteins encoded by *Shigella* strains have varied functions, but primary roles include facilitating invasion of epithelial cells and suppression of host immune responses including cytokine production.

Among animals used to model infection, only non-human primates develop shigellosis from oral inoculation (18); however, the expense of this model limits its utility. Several small animal models of *Shigella* infection have been developed, yet none capture all the features of natural human infection. Historically, the Sereny test was used to identify *Shigella* virulence factors required for induction of an inflammatory response (19); however, this ocular model bears little resemblance to natural infection. The adult rabbit ligated ileal loop model has proven useful for the study of *Shigella* virulence factors (20). However, this model bypasses the normal route of infection and challenges the small intestine, which is not the primary site of pathology in human infections. Intra-rectal guinea pig infection induces colonic pathology and bloody diarrhea (21), and has been used to dissect the contribution of *Shigella* and host factors in several aspects of pathogenesis (22–24). Adult mice, the most genetically tractable mammalian model organism, are recalcitrant to developing disease when inoculated orally (25). As an alternative to oral inoculation, an adult mouse pulmonary model of *Shigella* infection involving intranasal inoculation of mice with *Shigella* has been developed (26); this model provides a platform to investigate host immune responses and vaccine candidates (27, 28), and

has improved understanding of the innate immune response to *Shigella* infection (29). In contrast to adult mice, infant mice are susceptible to oral inoculation within a narrow window of time after birth, and inoculation with a high dose of the pathogen leads to mortality within a few hours; however, pathology is evident in the proximal small intestine rather than the distal small intestine or colon, and infected suckling mice do not develop diarrhea or intestinal fluid accumulation (30, 31). A zebrafish larvae model, in which the *Shigella* T3SS is required for pathogen virulence, has been useful for characterizing cell mediated innate immune responses to *Shigella* due to the ability to image infection in vivo (32, 33). Recently, an infant rabbit intra-rectal inoculation model was described in which animals develop disease and rectal pathology reminiscent of natural infections (10). The lack of a robust, oral inoculation-based, small animal model of shigellosis has limited understanding of the role of virulence factors in pathogenesis, particularly of the importance of such factors for enabling intestinal colonization and for generating pathology and clinical signs.

Here we found that oro-gastric inoculation of infant rabbits with *S. flexneri* results in severe disease resembling human shigellosis. Orally infected animals develop diarrhea and colonic pathology marked by damage to the epithelial cell layer and edema. Furthermore, the pathogen invaded and appeared to spread between colonic epithelial cells. We found that both the T3SS and IcsA were required for signs of disease, intestinal colonization and pathology. In addition, invasion of the pathogen into the epithelial cell layer was required for induction of host IL-8 expression. In situ mRNA labeling revealed that induction of IL-8 transcripts occurs primarily in cells adjacent to invaded epithelial cells, and not in the infected cells. Thus, our findings suggest that the oro-gastric infant rabbit model provides a powerful and accessible

small animal model for further investigation of factors contributing to *Shigella* pathogenesis and for testing new therapeutics.

Results

Infant rabbits develop diarrhea following oro-gastric inoculation with *S. flexneri*

In previous work, we found that oro-gastric inoculation of infant rabbits with Enterohemorrhagic *Escherichia coli* (EHEC), *Vibrio cholerae*, and *V. parahaemolyticus* (34–36) leads to diarrheal diseases and pathologies that mimic their respective human counterparts. Here, we explored the suitability of oro-gastric inoculation of infant rabbits to model *Shigella* infection. *S. flexneri* 2a strain 2457T, a human isolate that is widely used in the research community as well as in challenge studies in humans (37), was used in this work. We utilized a streptomycin resistant derivative of this strain for infections to facilitate enumeration of pathogen colony forming units (cfu) in samples from the rabbit intestine. This strain, which contains a point mutation resulting in a K43R mutation in the small (30S) ribosomal subunit protein RpsL, retains the full virulence plasmid and grows as well as the parent strain.

In order to investigate infant rabbits as a potential *Shigella* host, we orally inoculated two to three-day-old rabbits that were co-housed with their dam and then monitored for signs of disease. There was considerable variability in the development of diarrhea and colonization in initial studies using suckling rabbits fed ad libitum. Previous work using four-week-old rabbits suggested that a milk component could protect animals from disease by degrading the *Shigella* T3SS components (38, 39); consequently, additional experiments were performed with infant rabbits separated from their lactating dam for 24 hours prior to inoculation. Using this protocol, we obtained more reliable clinical disease and robust intestinal colonization. By 36 hours post infection (hpi), the majority (59%) of animals developed diarrhea, which was grossly visible as liquid fecal material adhering to the fur of the hind region of the rabbits (Fig. 1A-C), and high

levels of intestinal colonization (Fig. 2A); occasionally the diarrhea was frankly bloody. We chose the 36 hpi timepoint because from preliminary timecourse experiments we observed that all animals that were going to develop diarrhea developed disease by this timepoint and there was significant intestinal pathology at this time. Upon necropsy, the colon of infected animals was often bloody and contained liquid fecal material, in contrast to that of uninfected animals, which contained solid fecal pellets (Fig. 1D). Furthermore, some infected rabbits (27%) succumbed to infection rapidly and became moribund prior to 36 hpi, though not all of these animals developed diarrhea (Fig. 1A). Infected animals had highest bacterial burdens in the colon as well as the mid and distal small intestine (Fig 2A). The development of disease was associated with higher pathogen burdens in the colon (Fig. S1A). Separation of kits from the dam prior to inoculation led to a statistically significant elevation in intestinal colonization (Fig. S1B).

Although not all *S. flexneri* inoculated animals developed signs of disease, infected rabbits that developed diarrhea or died early displayed additional disease signs. The animals that developed disease had significantly lower body temperatures than uninfected animals (8-9°C lower than uninfected, Fig. 1E), and they had significantly smaller gains in body weight than infected animals without disease (-2% vs 13%) (Fig. 1F) over the course of the experiment. Despite the relatively large intra- and inter-litter variation in body weight, with a constant pathogen dose per animal ($1x10^9$ colony forming units, cfu), a lower initial body weight did not appear to be a risk factor for the development of disease (Fig. S1C).

Histopathologic examination of the intestines from infected rabbits revealed colonic pathology reminiscent of some of the features observed in infected human tissue, including

158 substantial edema (Fig. 2B) as well as sloughing of colonic epithelial cells (Fig. 2C). In unusual
159 cases, there was massive hemorrhage in the colonic tissue of infected rabbits (Fig. S2).
160 Uninfected rabbits, which were similarly fasted, did not display colonic pathology and had no
161 edema or disruption of the surface layer of epithelial cells (Fig. 2D). Notably, although the
162 bacterial burden in the colon was similar to that of the distal small intestine (Fig. 2A),
163 substantial pathology was not observed in the distal small intestine, suggesting organ-specific
164 host factors influence the development of intestinal pathology.
165
166 *S. flexneri* invades colonic epithelial cells after oro-gastric infection
167 Tissue sections from the colons of infected rabbits were examined with
168 immunofluorescence microscopy to determine the spatial distribution of *S. flexneri* in this
169 organ. The pathogen, which was labeled with an anti-*Shigella* antibody, was detected in the
170 intestinal lumen and in many scattered foci within the epithelium (Fig. 3AB). At low
171 magnification, the signal from the immunostained pathogen appeared to overlap with epithelial
172 cells (Fig. 3A-C). At high magnification, immunostained *S. flexneri* was clearly evident within the
173 boundaries of epithelial cells, which were visualized with phalloidin staining of actin and an
174 antibody against E-cadherin (Fig. 3D). Several *S. flexneri* cells were frequently observed within
175 an infected epithelial cell. In some infected epithelial cells, we observed *S. flexneri* cells
176 associated with phalloidin stained actin tails (Fig. 3E), and in other foci, we observed *S. flexneri*
177 in protrusions emanating from a primary infected cell with many cytosolic bacteria (Fig. 3F,
178 asterisk), similar to structures seen in *Shigella* infections of tissue cultured cells (40, 41). The
179 detection of actin tails and protrusions supports the hypothesis that the pathogen is actively

spreading within the epithelial cell layer in the colon. *S. flexneri* cells were primarily localized to the epithelial cell layer and were infrequently observed in the lamina propria, the region of the intestinal wall directly below the epithelial cell layer. We did not find bacteria in the deeper layers of the intestine (Fig. 3A). Hence, following oro-gastric inoculation of infant rabbits with *S. flexneri*, the pathogen appears to proliferate both within the colonic lumen and in epithelial cells without penetration into deeper tissues.

We also measured the burden of intracellular *S. flexneri* in the colon using a modified gentamicin protection assay previously used to study the intracellular burden of *Listeria monocytogenes* and *Salmonella enterica* serovar Typhimurium in murine intestinal tissues (42–46). After dissecting intestines from infected infant rabbits, colonic tissue was incubated with gentamicin, an antibiotic that selectively kills extracellular (i.e. luminal) bacteria. We observed an ~2 log decrease in bacterial burden after gentamicin treatment (Fig. 3G), suggesting that only a small portion of *S. flexneri* in the colon are intracellular.

IL-8 transcripts are often observed in epithelial cells near infected cells

We next investigated aspects of the infant rabbit host innate immune response to *S. flexneri* infection. IL-8, a proinflammatory CXC family chemokine that recruits neutrophils (47), has been shown to be elevated during *Shigella* infection in animal models (10, 21, 48) and in humans (49, 50). However, in preliminary experiments it was difficult to detect significant elevations of IL-8 transcripts in bulk colonic tissue using a qPCR-based assay. Due to the patchiness of the infection foci observed through immunofluorescence imaging of colonic tissue, we wondered whether a localized response to infection might be masked when

analyzing bulk intestinal tissue specimens. Local expression of IL-8 mRNA in *S. flexneri*-infected tissue was assessed using RNAscope technology, a sensitive, high-resolution in situ mRNA imaging platform that permits spatial analysis of mRNA expression. In the colon, we detected localized expression of IL-8 mRNA in colonic epithelial cells near infection foci (Fig. 4AB). In contrast, very few IL-8 transcripts were detected in the colons of uninfected kits (Fig. 4CD). Combined detection of IL-8 and *S. flexneri* demonstrated that IL-8 expressing cells were typically near cells containing *S. flexneri*, but not themselves infected with the pathogen (Fig. 4A, B & D, & S3). The majority (>90%) of infected epithelial cells did not express IL-8 mRNA, while >40% of these infected cells were adjacent to uninfected cells that did express IL-8 mRNA. Several T3SS effectors from *S. flexneri*, e.g. IpgD (51) and OspF (52), have been shown to reduce IL-8 expression in infected cells, which may explain the weak or absent IL-8 production in infected cells. There was a wide range in the prevalence of IL-8 producing cells in infected animals (Fig. 4D & S3). The variability of IL-8 expression after infection may reflect the patchiness of *S. flexneri* invasion along the colon (Fig. 3A). Together, these observations suggest that *S. flexneri* infection induces IL-8 mRNA expression (and perhaps additional cytokines as well) in infant rabbits.

Narrow bottleneck to *Shigella* infection of the infant rabbit colon

We attempted to use transposon-insertion sequencing (TIS) to identify genetic loci contributing to *S. flexneri* colonization and pathogenesis, as we have done with *V. cholerae* (53, 54), *V. parahaemolyticus* (55), and EHEC (56). Initially, a high-density transposon mutant library in *S. flexneri* was created using a *mariner*-based transposon that inserts at TA dinucleotide sites

in the genome. The library included insertions across the entirety of the genome, including the virulence plasmid (Table S1). Infant rabbits were inoculated with the transposon library and transposon mutants that persisted after 36 hpi were recovered from the colon. Comparison of the frequencies of insertions in the input and output libraries revealed that the output transposon libraries recovered from rabbit colons only contained ~20% of the transposon mutants that were present in the input library. These observations suggest that there is a very narrow bottleneck for *S. flexneri* infection in rabbits, leading to large, random losses of diversity in the input library. These random losses of mutants confound interpretation of these experiments and precludes accurate identification of genes subject to in vivo selection. Modifications to the in vivo TIS protocol will be necessary to apply TIS to identify additional *S. flexneri* colonization factors.

Canonical *S. flexneri* virulence factors are required for intestinal colonization and pathogenesis

Next, we investigated the requirement for canonical *Shigella* virulence factors in intestinal colonization and disease pathogenesis. First, we tested a strain that lacked the entire virulence plasmid, which contains most of the known virulence factors encoded in the *S. flexneri* genome, including the T3SS. As anticipated, this strain was avirulent; animals inoculated with the plasmid-less (plasmid -) *S. flexneri* strain did not die or develop diarrhea or reduced temperature (Fig. 1A & E). We also tested isogenic mutants that lack one of two key virulence factors: IcsA (Δ*icsA* strain), which is required for intracellular actin-based motility and cell-to-cell spreading, and MxiM (Δ*mxiM* strain), which is a T3SS structural component (57). *MxiM* deletion mutants do not assemble a functional T3SS, do not secrete T3SS effectors, and do not invade

246 tissue-cultured epithelial cells (57–59). Like the plasmidless strain, the Δ*icsA* and Δ*mxiM* strains
247 did not cause disease; none of the rabbits infected with either of these two mutant strains
248 developed diarrhea, succumbed to infection, or had a reduction in body temperature (Fig. 1A &
249 E). Additionally, none of the mutants induced colonic edema or epithelial cell sloughing,
250 pathologic features that characterized WT infection (Fig. 2 and Fig. 6). Collectively, these data
251 indicate that both IcsA and the T3SS are required for *Shigella* pathogenesis in the infant rabbit
252 model.

253 All three of the mutant strains had reduced capacities to colonize the infant rabbit
254 intestine (Fig. 5). Notably, the reduction in the colonization of the *icsA* mutant was at least as
255 great as the other two mutant strains, suggesting that cell-to-cell spreading or the adhesin
256 function of IcsA is critical for intestinal colonization. The colonization defects were most
257 pronounced in the small intestine, where up to 10^4-fold reductions in recoverable *S. flexneri* cfu
258 were observed (Fig. 5). Reductions in the colon were less marked and did not reach statistical
259 significance for the Δ*mxiM* strain (Fig. 5).

260 Interestingly, the *icsA* mutant led to an accumulation of heterophils (innate immune
261 cells that are the rabbit equivalent of neutrophils) in the colon that was not observed in animals
262 infected with the WT strain (Fig. 6). Thus, IcsA may contribute to immune evasion by limiting
263 the recruitment of innate immune cells. The *mxiM* mutant also recruited more heterophils to
264 the lamina propria and epithelial cell layer than the WT strain (Fig. 6A & C). Unlike the Δ*icsA* and
265 Δ*mxiM* strains, the plasmidless strain did not recruit heterophils in the colon. Thus, both IcsA
266 and the T3SS appear to antagonize heterophil recruitment, perhaps by facilitating pathogen
267 invasion. However, the absence of heterophil influx in the plasmidless strain challenges this

hypothesis and suggests that another plasmid-encoded factor can counteract the actions of IcsA and/or the T3SS in blocking heterophil infiltration.

Since colonic pathology was altered in the mutant strains, we investigated the intestinal localization and IL-8 production induced by the mutants. All three of the mutant strains were found almost exclusively in the lumen of the colon (Fig. 7A, Fig. S4); in contrast to the WT strain (Fig. 3), it was difficult to detect infection foci in the epithelial cell layer in animals infected with mutant strains (Fig. 7). The *icsA* mutant was occasionally observed inside epithelial cells (Fig 7B), but larger foci were not detected. As expected, we observed very few cells expressing IL-8 mRNA in the colons of rabbits infected with any of the three mutant *S. flexneri* strains (Fig. 4D & 7B), supporting the idea that induction of IL-8 expression requires *S. flexneri* invasion of the epithelial cell layer in this model.

Discussion

Small animal models of shigellosis that rely on the oral route of infection have been lacking. Here, we found that oro-gastric inoculation of two to three-day-old infant rabbits with *S. flexneri* led to a diarrheal disease and colonic pathology reminiscent of some aspects of human disease. Fasting animals prior to inoculation reduced the variability in infection outcomes, but not all inoculated animals developed disease. The pathogen robustly colonized the colon, where the organism was found primarily in the lumen; however, prominent infection foci were also observed within the colonic epithelium. Robust *S. flexneri* intestinal colonization, invasion of the colonic epithelium and colonic epithelial sloughing required IcsA and the T3SS, which are both canonical *S. flexneri* virulence factors. Despite the reduced intestinal colonization of the *icsA* and *mxiM* mutants, these strains elicited more pronounced colonic inflammation (characterized by infiltration of heterophils) than the WT strain. IL-8 expression, detected with in situ mRNA labeling, was higher in animals infected with the WT versus the mutant strains, suggesting that epithelial invasion promotes expression of this chemokine. Interestingly, IL-8 expression was greater in uninfected cells near infected epithelial cells than in infected epithelial cells themselves. Collectively, our findings suggest that oral infection of infant rabbits offers a useful experimental model for investigations of the pathogenesis of shigellosis.

Fasted animals developed disease more frequently and had elevated intestinal colonization compared to animals who fed ad libidum prior to inoculation. The presence of inhibitory substances in milk, such as lactoferrin, which degrades components of the *Shigella* T3SS apparatus (39), may limit bacterial establishment in the intestine, but have less potent

effects once colonization is established. Mean colonic colonization was higher in animals that developed disease than those that did not (Fig S1A). However, high bacterial burdens are not the only factor predictive of disease; several animals with high pathogen burdens did not exhibit signs of disease (Fig. S1A). Also, initial rabbit body weights did not strongly influence clinical outcomes (Fig. S1C). Several additional factors likely modulate *Shigella* colonization and disease manifestation in infant rabbits. For example, variations in the intestinal microbiota of the infant rabbits may limit or potentiate *S. flexneri* virulence and/or colonization, as described for infections caused by other enteric pathogens, including *Clostridium difficile* (60), *L. monocytogenes* (61), and *V. cholerae* (62). Differences in dam feeding patterns also likely influence colonization and disease outcomes. Further elucidation of factors that modulate outcomes will be valuable to improve this model because they may point to ways to elevate the fraction of animals that develop clinical signs of infection.

A high inoculum dose (10^9 cfu) was required to achieve reliable disease development following oral inoculation of two to three-day-old infant rabbits. Animals inoculated with lower doses (e.g., 10^7 cfu) of *S. flexneri* developed disease and robust intestinal colonization at lower frequencies. Interestingly, even in oral non-human primate models, the standard inoculum dose (10^{10} cfu) to ensure consistent development of disease (63, 64) is orders of magnitude greater than the dose used in human challenge studies (typically 10^3-10^4 cfu) (37, 65, 66). The reasons accounting for these marked differences in infectious doses warrant further exploration. It is unlikely that older rabbits infected via the oral route will be susceptible to colonization and disease, since our findings with other pathogens (35) suggest that infant rabbits become resistant to oral inoculation with enteric pathogens when they are ~5 days old.

In human infections, *Shigella* causes colonic pathology characterized by an acute inflammatory response with mucosal ulceration and erosions, neutrophil infiltration, congestion, and hemorrhage (8, 9). In the oral infant rabbit model, the WT strain caused edema and sloughing of epithelial cells in the colon, but we did not observe recruitment of heterophils, suggesting that colonic pathology is not primarily attributable to an acute inflammatory response characterized by heterophil infiltration. Instead, the pathology may be driven by invasion and replication of the pathogen within colonic epithelial cells. Oro-gastric inoculation of infant rabbits with EHEC induces heterophil infiltration in the colon (67), indicating that these animals are capable of mounting an acute inflammatory response in this organ.

The marked colonization defect of the Δ*icsA* strain, matching that observed for the Δ*mxiM* (T3SS -) and plasmidless strains, was unexpected. It seems unlikely the Δ*icsA* mutant's colonization defect is entirely attributable to the mutant's deficiency in cell-to-cell spreading. Zumsteg et al. found that IcsA can also serve as an adhesin (68). Since distinct regions of IcsA are required for its adhesive versus cell spreading activities (68), it may be possible to genetically dissect which of these IcsA functions plays a dominant role in colonization, using *S. flexneri* strains producing mutant versions of IcsA. Passage of the pathogen through the upper gastrointestinal tract may be required to reveal IcsA's adhesive activity, because a Δ*icsA* strain had only a modest colonization defect after intra-rectal instillation (10). It was also surprising that the animals infected with the Δ*icsA* strain recruited heterophils to the colon despite little induction of IL-8 expression. These observations suggest that there are additional factors contributing to heterophil recruitment to the rabbit colon. Moreover, since there is minimal heterophil recruitment in animals infected with the WT strain, IcsA-mediated pathogen

adherence to colonic epithelial cells (and potentially concomitant increased invasion) may increase delivery of T3SS effectors into host cells, thereby repressing a host-derived heterophil recruitment factor.

Our attempts to utilize TIS to identify novel genetic loci contributing to *S. flexneri* colonization in the infant rabbit intestine were stymied by a narrow infection bottleneck. The tight bottleneck leads to large, random losses of genetic diversity of the input library. The underlying causes of in vivo bottlenecks vary and may include stomach acidity, host innate immune defenses, such as antimicrobial peptides, the number of available niches in the intestine, and competition with the endogenous commensal microbiota (69). Modifications to either the inoculation protocol or library generation could facilitate future in vivo TIS screens. For example, the diversity of the inoculum could be reduced by generating a defined library of transposon mutants with only one or two mutants per gene (e.g. as has been done in *Edwardsiella piscicida* (70)). Regarding the infection protocol, it is possible that the fraction of the inoculum that initially seeds and colonizes the intestine could be elevated by reducing the number of commensal organisms in the intestine that may compete for a niche similar to that occupied by *S. flexneri*. Similar strategies have been utilized to facilitate studies of other enteric pathogens (71, 72).

The intra-rectal infant rabbit model of shigellosis reported by Yum et al. has some beneficial features compared to the oral infection model. Using this route, Yum et al. reported that all animals developed bloody diarrhea and colonic pathology that included substantial recruitment of heterophils (10). As noted above, for unknown reasons, oral inoculation of WT *S. flexneri* did not lead to heterophil recruitment to sites of damage in the colon. An additional

367 difference is that intra-rectal instillation of a Δ*icsA* mutant led to induction of cytokine
368 expression, heterophil recruitment, and only slightly reduced colonization of the strain,
369 whereas following oral inoculation, a Δ*icsA S. flexneri* exhibited a marked colonization defect
370 and did not induce IL-8 mRNA expression. Additional studies are required to elucidate the
371 reasons that account for the differential importance of IcsA in these models. While some
372 features of the intra-rectal model are attractive, Yum et al. used 2 week old rabbits that were
373 carefully hand reared in an animal facility from birth using a complex protocol that may prove
374 difficult for others to adopt (10). In addition to the physiologic route of infection, the oral infant
375 rabbit model requires far less specialized animal husbandry than the intra-rectal model and
376 may therefore prove more accessible.

377 In summary, oral inoculation of infant rabbits with *Shigella* provides a feasible small
378 animal model to study the pathogenesis of this globally important enteric pathogen. The model
379 should also be useful to test new therapeutics for shigellosis, an issue of increasing importance
380 given the development of *Shigella* strains with increasing resistance to multiple antibiotics (73–
381 76).

382 **Figure Legends**

383

384 **Figure 1. Clinical signs and gross pathology of infant rabbits following oro-gastric inoculation**

385 **of *S. flexneri*.**

386 A. Clinical signs in infant rabbits infected with *S. flexneri* or isogenic mutant strains. Statistical

387 significance for development of diarrhea between the animals in the WT group and in each of

388 the other groups was determined using a Fisher's exact test.

389 B-C. Hind regions of animals inoculated with the WT strain (B) or an uninfected animal (C).

390 Arrows indicate liquid feces stuck on anus and hind paws.

391 D. Colons from animals inoculated with the WT strain (left) or of an uninfected animal (right).

392 Arrowheads point to regions of liquid feces and arrows indicate solid fecal pellets.

393 E. Body temperature of animals inoculated with the indicated strains 36 hpi or when they

394 became moribund. Standard error of the mean values are superimposed. Disease +/- indicates

395 whether or not animals developed diarrhea or became moribund early; all groups were

396 compared to the WT (diarrhea +) group using a Kruskal-Wallis test with Dunn's multiple-

397 comparison. p-values: <0.05, *; <0.01, **; <0.001, ***.

398 F. Percentage change in weight of infant rabbits infected with the WT strain, grouped by

399 whether or not they developed disease (+/-). Percentage change in weight is calculated as

400 difference between the final weight of the animal at 36 hpi or the last weight measurement

401 taken when they became moribund (final) and the initial weight of the animal upon arrival in

402 the animal facility (initial). Means and standard error of the mean values are superimposed.

403 Groups were compared with a Mann-Whitney U test. p-values: <0.05, *.

Figure 2. Intestinal colonization and colonic pathology in infant rabbits infected with *S. flexneri*.

A. Bacterial burden of *S. flexneri* in the indicated intestinal sections 36 hpi; SI = small intestine. Each point represents measurement from one rabbit. Data plotted as log transformed colony forming units (cfu) per gram of tissue; mean values are indicated with bars. Open circles represent the limit of detection of the assay and are shown for animals where no cfu were recovered.

B-D. Representative haematoxylin and eosin-stained colonic sections from infected animals (B,C) 36 hpi or uninfected animals (D). Arrowheads in (B) indicate areas of edema in the lamina propria. Arrowheads in (C) indicate areas where the epithelial cell layer is absent. Arrows in (D) point to the intact layer of epithelial cells seen in the colon. The dashed lines indicate the presence (inset, D) or absence (inset, C) of the epithelial cell layer. Scale bar is 100 µm.

Figure 3. Localization of *S. flexneri* in the colons of infected infant rabbits.

A-F. Immunofluorescence micrographs of *S. flexneri* in colonic tissue of infected rabbits 36 hpi. (A) *S. flexneri* bacteria were found in large numbers in epithelial foci (A, arrowheads point to selected foci). Scale bar is 500 µm. (B) *S. flexneri* bacteria in the lumen of the colon; the intestinal lumen and intestinal wall are labeled. Scale bar is 500 µm. (C) Arrowheads show infection foci where multiple neighboring cells contain intracellular *S. flexneri*. Scale bar is 100 µm. (D) Immunofluorescence z-stack micrograph of *S. flexneri* within colonic epithelial cells. Scale bar is 10 µm. Left (square) panel shows xy plane at a single z position, indicated by the

horizontal axis of the cross-hairs in the yz projection. Right (rectangular) panel shows yz projection along the plane indicated by the vertical axis of the cross-hairs in the xy plane. Scale bar is 10 µm. (E) Immunofluorescence micrograph of *S. flexneri* associated with actin tails within colonic epithelial cells. Arrows point to poles of *S. flexneri* bacterial cells from which the actin tail is formed. Scale bar is 10 µm. (F) Immunofluorescence micrograph of *S. flexneri* forming protrusions during cell-to-cell spread between colonic epithelial cells. Asterisk marks a likely primary infected cell. Scale bar is 10 µm. Panels show zoomed region of phalloidin or anti-*Shigella* channels. Scale bar is 5 µm. Arrow points to actin surrounding the bacterial cell in a protrusion, arrowheads indicate the actin tail and actin cytoskeleton inside the protrusion at the pole of the bacterial cell and at the base of the protrusion. Blue, DAPI; green, FITC-conjugated anti-*Shigella* antibody; red (A-C or magenta in D-F), phalloidin-Alexa 568; and when present, red (D), anti-E-cadherin.

G. Bacterial burden of *S. flexneri* WT strain in the indicated intestinal sections 36 hpi. Each point represents measurement from one rabbit. Data plotted as log transformed colony forming units (cfu) per gram of tissue; means and standard error of the mean values are superimposed. Open symbols represent the limit of detection of the assay and are shown for animals where no cfu were recovered. Statistical significance was determined with a Kruskal-Wallis test with Dunn's multiple comparison. p-values: <0.05, *; <0.01, **.

Figure 4. Colonic IL-8 mRNA in rabbits infected with *S. flexneri*.

A-C. Immunofluorescence micrographs of colonic sections from infant rabbits infected with WT *S. flexneri* (A, B) or uninfected control (C). Sections were stained with an RNAscope probe to

448 rabbit IL-8 (red), an antibody to *Shigella* (FITC-conjugated anti-*Shigella* green), and with DAPI
449 (blue). (A) Colon section infected with WT *S. flexneri.* Inset on right of A depicts magnified view
450 of boxed area on left image. Scale bar is 200 µm. (B) High magnification of colonic epithelium
451 infected with WT *S. flexneri.* Sections were also stained with anti-E-cadherin antibody
452 (magenta). Scale bar is 10 µm. (C) Uninfected colon section. Scale bar is 100 µm.
453 D. Percentage of IL-8 expressing cells in each field of view from colonic tissue sections stained
454 with probe to rabbit IL-8 from rabbits infected with the indicated strain. See methods for
455 additional information regarding the determination of these measurements. Mean values are
456 indicated with bars. All groups were compared to the sections from the uninfected animals.
457 Statistical significance was determined using a Kruskall-Wallis test with Dunn's multiple
458 comparison. P-values: <0.001, ***.
459
460 **Figure 5. Intestinal colonization of WT and mutant *S. flexneri*.**
461 A-E. Bacterial burden of the indicated strains in the indicated intestinal sections 36 hpi. SI =
462 small intestine. Each point represents measurement from one rabbit. Data plotted as log
463 transformed colony forming units (cfu) per gram of tissue. Means and standard error of the
464 mean values are superimposed. Open symbols represent the limit of detection of the assay and
465 are shown for animals where no cfu were recovered. For each section, burdens from all strains
466 were compared to each other; statistical significance was determined using a Kruskal-Wallis
467 test with Dunn's multiple comparison. P-values: <0.05, *; <0.01, **; <0.001, ***; <0.0001, ****.
468
469 **Figure 6. Colonic pathology in rabbits infected with WT or mutant *S. flexneri*.**

A. Histopathological scores of heterophil infiltration in colonic sections of animals infected with indicated strains of *S. flexneri*. Means and standard error of the mean values are superimposed. Statistical significance was determined using a Kruskal-Wallis test with Dunn's multiple comparison; comparisons that are non-significant are not labeled.

B-D. Representative haematoxylin and eosin-stained colonic sections from rabbits infected with the indicated strains 36 hpi. In B, the inset on the right displays the magnified version of the boxed region of the larger micrograph. Arrowheads point to heterophils (pink cytoplasm, multi-lobular darkly stained nucleus). Scale bar is 100 µm. In C (MxiM mutant), the inset on the right displays a magnified version of the boxed region of the larger micrograph. Arrowheads point to heterophils. Scale bar is 100 µm.

Figure 7. Intestinal localization and IL-8 transcripts in colons from animals infected with an *icsA* mutant.

A. Immunofluorescence micrograph of Δ*icsA* in colonic tissue of infected rabbits 36 hpi. Blue, DAPI; green, FITC-conjugated anti-*Shigella* antibody; red, phalloidin-Alexa 568. Scale bar is 500 µm.

B. Immunofluorescence micrograph of sections stained with a RNAscope probe to rabbit IL-8 (red), antibodies to *Shigella* (green) and E-cadherin (magenta), and DAPI (blue). Panels on right depicts channels of merged left image. Arrows point to multiple *icsA* bacteria in the cytoplasm of two infected cells. Scale bar is 10 µm.

Acknowledgements

This study was supported by the NIGMS grant T32GM007753 (J.D.D.), NIAID grant T32AI-132120 (J.D.D. & A.R.W.), and NIAID grant R01-AI-043247 and the Howard Hughes Medical Institute (M.K.W.).

We gratefully acknowledge Marcia Goldberg for providing *S. flexneri* 2a strains 2457T and BS103 (the virulence plasmidless derivative), and for transducing the streptomycin resistance allele into BS103. We thank Angelina Winbush for help with construction of the Δ*icsA* mutant strain. We thank the Dana-Farber/Harvard Cancer Center in Boston, MA, for the use of the Rodent Histopathology Core, which provided tissue embedding, sectioning, and staining service (NIH 5 P30 CA06516). We thank Rod Bronson at the Rodent Histopathology Core for providing blinded pathology scoring of tissue sections. We thank Brigid Davis and members of the Waldor lab for comments on the manuscript.

Materials and Methods

Bacterial strains and growth

Bacterial strains are listed in Table S2. *S. flexneri* were routinely grown aerobically in Miller lysogeny broth (LB) or LB agar at 30°C or 37°C. Antibiotics, when used, were included at the following concentrations: Streptomycin (Sm) 200 µg/mL, Kanamycin (Km) 50 µg/mL, Carbenicillin (Carb) 100 µg/mL, Chloramphenicol (Cm) 10 µg/mL. To check for the presence of the virulence plasmid, bacteria were grown on media with Congo red added at 0.1% w/v.

E. coli were routinely grown in LB media or agar. Antibiotics were used at the same concentrations as *S. flexneri* except for Cm, which was 30 µg/mL. When required, di-aminopimelic acid (DAP) was added at a concentration of 0.3 mM.

Strain construction

S. flexneri 2a strain 2457T and BS103 (a derivative lacking the virulence plasmid) were gifts of Marcia Goldberg. A spontaneous streptomycin resistant strain of *S. flexneri* 2a strain 2457T was generated by plating overnight LB cultures of *S. flexneri* 2a 2457T on 1000 µg/mL Sm LB plates and identifying Sm resistant (Sm^R) strains that grew as well as the parent strain. The Sm^R strain was used as the wild type strain for all subsequent experiments, including animal experiments and construction of mutant strains. Primers (Table S2) were used to amplify the *rpsL* gene in the strain and Sanger sequencing was performed to determine the nature of the mutation resulting in streptomycin resistance. The streptomycin resistance allele was transferred from the Sm^R wild type strain into strain BS103 by P1 transduction, yielding a Sm^R plasmidless (plasmid -) strain.

Single gene deletion mutants were generated in the WT Sm^R strain using the lambda red recombination method, as previously described (77). Resistance cassettes used in the process

were amplified from pKD3 (Cm). Mutations generated by lambda red were moved into a clean genetic background by transferring the mutation to the Sm^R wild type strain via P1 transduction. Subsequently, antibiotic resistance cassettes were removed via FLP-mediated recombination using pCP20. Retention of the virulence plasmid throughout P1 transduction of the mutation into the parental WT Sm^R strain was monitored by plating bacterial mutants on LB + Congo Red to identify red colonies, and by performing multiplex PCR for various genes spread across the virulence plasmid – primers are listed in Table S2.

Animal Experiments

Rabbit experiments were conducted according to the recommendations of the National Institutes of Health Guide for the Care and Use of Laboratory Animals, the Animal Welfare Act of the United States Department of Agriculture, and the Brigham and Women's Hospital Committee on Animals, as outlined in Institutional Animal Care and Use Compliance protocol #2016N000334 and Animal Welfare Assurance of Compliance number A4752-01.

Litters of two to three-day-old New Zealand White infant rabbits with lactating adult female (dam) obtained from a commercial breeder (Charles River, Canada or Pine Acres Rabbitry Farm & Research Facility, Norton, MA) were used for animal experiments.

Infant rabbits were administered a subcutaneous injection of Zantac (ranitidine hydrochloride, 50 mg/kg; GlaxoSmithKline) 3 hours prior to inoculation with the wild type (Sm^R) or isogenic mutants. We attempted to utilize a bicarbonate solution to administer bacteria, but found that *S. flexneri* do not survive when re-suspended in a sodium bicarbonate solution. For initial experiments, a day after arrival, infant rabbits were oro-gastrically inoculated with 1e9 cfu of log phase *S. flexneri* suspended in LB. To prepare the inoculum, an overnight bacterial

550 culture grown at 30°C was diluted 1:100 and grown at 37°C for 3 hours. The bacteria were
551 subsequently pelleted and re-suspended in fresh LB to a final concentration of 2e9 cfu/mL.
552 Rabbits were oro-gastrically inoculated using a PE50 catheter (Becton Dickson) with 0.5 mL of
553 inoculum (1e9 cfu total). In later experiments, infant rabbits were first separated from the dam
554 for 24 hours prior to inoculation, after which they were immediately returned to the dam for
555 the remainder of the experiment.

556 The infant rabbits were then observed for 36-40 hours post-inoculation and then
557 euthanized via isoflurane inhalation and subsequent intracardiac injection of 6 mEq KCl at the
558 end of the experiment or when they became moribund. Animals were checked for signs of
559 disease every 10-12 hours. Body weight and body temperature measurements were made 1-2
560 times daily until the end of the experiment. Body temperature was measured with a digital
561 temporal thermometer (Exergen) and assessed on the infant rabbit chest, in between the front
562 legs. Temperatures reported in Figure 1E are the final temperatures prior to euthanasia and
563 change in body weight in Figure 1F is a comparison of the final to initial body weight. Diarrhea
564 was scored as follows: no diarrhea (solid feces, no adherent stool on hindpaw region) or
565 diarrhea (liquid fecal material adhering to hindpaw region). Animal experiments with isogenic
566 mutants were always conducted with litter-mate controls infected with the WT Sm^R strain to
567 control litter variation.

568 At necropsy, the intestine from the duodenum to rectum was dissected, and divided
569 into separate anatomical sections (small intestine, colon) as previously described (54, 78). 1-2
570 cm pieces of each anatomical section were used for measurements of tissue bacterial burden.
571 Tissue samples were placed in 1x phosphate buffered saline (PBS) with 2 stainless steel beads

572 and homogenized with a bead beater (BioSpec Products Inc.). Serial dilutions were made using
573 1xPBS and plated on LB+Sm media for enumeration of bacterial cfu. For processing of tissue for
574 microscopy, 1-2 cm pieces of the tissue adjacent to the piece taken for enumeration of bacterial
575 cfu were submerged in either 4% paraformaldehyde (PFA) for frozen sections or 10% neutral-
576 buffered formalin (NBF) for paraffin sections.

577 For gentamicin tissue assays, a 1-2 cm portion of the colon was cut open longitudinally
578 and washed in 1X PBS to remove luminal contents and then incubated in 1mL of 1xDMEM with
579 100 µg/mL gentamicin for 1 hour at room temperature. The tissue was subsequently washed 3x
580 with 20x volumes of 1x PBS for 30 min with shaking. The tissue was then homogenized and
581 serial dilutions were plated on LB+Sm media for enumeration of bacterial burden.

582 For Tn-seq experiments, aliquots of the transposon library were thawed and aerobically
583 cultured in LB for 3 hours. The bacteria were pelleted and resuspended in fresh LB to a final
584 concentration of 1e9 cfu per 0.5 mL inoculum. A sample of the input library (1e10 cfu) was
585 plated on a large LB+Sm+Km plate (245 cm^2; Corning). Bacterial burdens in infected rabbit
586 tissues were determined by plating serial dilutions on LB+Sm+Km plates. The entire colon was
587 homogenized and plated onto a large LB+Sm+Km plate to recover transposon mutants that
588 survived in the colon. Bacteria on large plates were grown for ~20-22 hours at 30°C, scraped off
589 with ~10 mL fresh LB, and ~ 1 mL aliquots were pelleted. The pellets were frozen at -80°C prior
590 to genomic DNA extraction for Tn-seq library construction.

591 Data from animal experiments were analyzed in Prism (ver. 8; GraphPad). The Mann-
592 Whitney U test or the Kruskal-Wallis test with Dunn's post-test for multiple comparisons were

593 used to compare the tissue bacterial burdens. A Fisher's exact test was used to compare the
594 proportion of rabbits that developed diarrhea after infection with various bacterial strains.

595

596 Immunofluorescence Microscopy

597 Immunofluorescence images were analyzed from 20 wild-type and at least 4 rabbits
598 infected with each of the various mutant bacterial strains, or uninfected rabbits; 2-3 colon
599 sections per rabbit were examined. Tissue samples used for immunofluorescence were fixed in
600 4% PFA, and subsequently stored in 30% sucrose prior to embedding in a 1:2.5 mixture of OCT
601 (Tissue-Tek) to 30% sucrose and stored at -80°C, as previously described (35). Frozen sections
602 were made at 10 µm using a cryotome (Leica CM1860UV). Sections were first blocked with 5%
603 bovine serum albumin (BSA) in PBS for 1 hour. Sections were stained overnight at 4°C with a
604 primary antibody, diluted in PBS with 0.5% BSA and 0.5% Triton X-100: anti-*Shigella*-FITC
605 (1/1000; #0903, Virostat); anti-E-cadherin 1:100 (610181, BD Biosciences). After washing with
606 1xPBS - 0.5% Tween20 (PBST), sections were incubated with 647 phalloidin (1/1000; Invitrogen)
607 for 1 hour at room temperature, washed and stained for 5 min with 4',6-diamidino-2-
608 phenylindole (DAPI) at 2 µg/mL for 5 min, and covered with ProLong Diamond or Glass Antifade
609 (Invitrogen) mounting media. Slides were imaged using a Nikon Ti Eclipse equipped with a
610 spinning disk confocal scanner unit (Yokogawa CSU-Xu1) and EMCCD (Andor iXon3) camera, or
611 with a sCMOS camera (Andor Zyla) for widefield microscopy.

612

613 Histopathology

614 Tissue samples used for histopathology analysis were fixed in 10% NBF and
615 subsequently stored in 70% ethanol prior to being embedded in paraffin, as previously
616 described (36). Formalin fixed, paraffin embedded (FFPE) sections were made at a thickness of

617 5 µm. Sections were stained with hematoxylin and eosin (H&E). Slides were assessed for various
618 measures of pathology, e.g. heterophil infiltration, edema, epithelial sloughing, hemorrhage, by
619 a pathologist blinded to the tissue origin. Semi-quantitative scoring for heterophil infiltration
620 were as follows: 0, no heterophils observed; 1, rare heterophils; 2, few heterophils; 3, many
621 heterophils; 4, abundant heterophils. Brightfield micrographs were collected using an Olympus
622 VS120.

623
624 In situ RNA hybridization
625 Freshly cut FFPE sections (5 µm) were made of the indicated anatomical sections and
626 stored with desiccants at 4°C. Subsequently, sections were processed and analyzed using the
627 RNAscope Multiplex Fluorescent v2 Assay (Advanced Cell Diagnostics USA-ACDbio) combined
628 with immunofluorescence. Briefly, sections were processed following ACDbio
629 recommendations for FFPE sample preparation and pretreatment using 15-minute target
630 retrieval and 25-minute Protease Plus digestion using the RNAscope HybEZ oven for all
631 incubations. An RNAscope C1 probe (OcIL8) to rabbit CXCL8 was developed and used to stain
632 intestinal sections for CXCL8 mRNA expression. C1 probe was detected with Opal 570 dye
633 (Akoya Biosciences) diluted 1:1000 in Multiplex TSA buffer (ACDbio). Sections were also stained
634 with DAPI (2 µg/mL), anti-*Shigella* FITC (1/1000, Virostat), and anti-mouse E-cadherin (1/100;
635 #610181, BDbiosciences). Slides were imaged using a Nikon Ti Eclipse equipped with a spinning
636 disk confocal scanner unit (Yokogawa CSU-Xu1) and EMCCD (Andor iXon3) camera for high
637 magnification images. Slides were imaged using a widefield Zeiss Axioplan 2 microscope
638 through the MetaMorph imaging system for RNAscope signal quantification.

639
640 Quantitative Image Analysis

Images of mid colon tissue sections stained with RNAscope OcIL8, DAPI, and FITC-conjugated anti-*Shigella* antibody were acquired and analyzed using the MetaMorph (7.1.4.0) application. Briefly, tiled 10x images covering the entire length of the tissue section were collected using Multi-Dimensional Acquisition. For analysis of the percentage of IL-8 mRNA expressing cells that were adjacent to infected cells, we analyzed 86 foci of infection at 100x magnification. Exclusive threshold values were set for the DAPI channel or the rhodamine channel independently and applied to all images in the data set. The threshold values for DAPI or rhodamine were used to create a binary mask of each image. The total area under the binary mask was recorded and used to calculate the percent of total tissue (DAPI area under mask) expressing CXCL8 mRNA (rhodamine area under mask) by dividing the values for rhodamine area by the DAPI area for each image. Percentages were graphed using Prism version 8 (GraphPad).

Transposon library construction and analysis

A transposon library was constructed in *S. flexneri* 2a 2457T Sm^R (WT Sm^R) using pSC189 (79), using previously described protocols (54, 80) with additional modifications. Briefly, *E. coli* strain MFD*pir* (81) was transformed with pSC189. Conjugation was performed between WT Sm^R and MFD*pir* pSC189. Overnight LB cultures of WT Sm^R (grown at 30°C) and MFD*pir* (grown at 37°C) were mixed and spotted onto 0.45 µm filters on LB+DAP agar plates. The conjugation reaction was allowed to proceed for 2 hours at 30°C. Subsequently, the bacterial mixtures were resuspended in LB and spread across four 245 cm^2 LB+Sm+Km square plates to generate single separate colonies for a transposon library. The square plates were grown at 30°C for 20 hours. The colonies that formed (~800,000 total) were washed off with LB (8 mL per plate) and the

664 bacteria from two plates were combined. Two separate 1 mL aliquots of the two combined
665 mixtures were used to start two 1000 mL LB+Km liquid cultures. The cultures were grown
666 aerobically at 30°C with shaking for 3 hours. For each flask, the bacteria were pelleted and
667 resuspended in a small amount of LB before being spread across two 245 cm^2 LB+Sm+Km
668 square plates and grown at 30°C for 20 hours. The resulting bacteria on the plate were washed
669 off with LB and resuspended. The OD was adjusted to 10 with LB and glycerol so that the final
670 concentration of glycerol was 25%. 1 mL LB + glycerol aliquots were stored at -80°C for later
671 experiments. In addition, 1 mL aliquots were also pelleted, to generate bacterial pellets to serve
672 as sources of genomic DNA for the initial characterization of the transposon library. The pellets
673 were stored at -80°C prior to genomic DNA extraction for Tn-seq library construction.
674 Tn-seq library construction and data analysis was performed as previously described
675 (54, 55, 82); briefly, genomic DNA was extracted, transposon junctions were amplified,
676 sequencing was performed on an Illumina MiSeq, and data were analyzed using a modified
677 ARTIST pipeline (54, 55). Sequence reads were mapped onto the *S. flexneri* 2a strain 2457T
678 chromosome (Refseq NC_004741.1) and *S. flexneri* 2a strain 301 virulence plasmid (Refseq
679 NC_004851.1). Reads at each TA site were tallied.

680 **Supplemental Figure Legends**

681

682 **Figure S1. Factors influencing development of diarrheal disease in infant rabbits after oro-**
683 **gastric inoculation of *S. flexneri*.**

684 A-B. Bacterial burden of *S. flexneri* in the indicated intestinal sections 36 hpi; SI = small
685 intestine. Each point represents measurement from one rabbit. Data plotted as log transformed
686 colony forming units (cfu) per gram of tissue. Means and standard error of the mean values are
687 superimposed. Open circles represent the limit of detection of the assay and are shown for
688 animals where no cfu were recovered. (A) 'disease +' refers to animals infected with the WT *S.*
689 *flexneri* strain that developed disease (diarrhea or became moribund early), 'disease -' refers to
690 animals infected with the WT *S. flexneri* strain that did not develop disease. (B) 'unfasted' refers
691 to animals fed ad libitum prior to inoculation, 'fasted' refers to animals separated from dams
692 for 24 hours prior to inoculation.
693 C. Initial body weights of infant rabbits inoculated with WT *S. flexneri*, grouped based on
694 whether animal developed disease (diarrhea or early mortality). Means and standard error of
695 the mean values are superimposed.

696

697 **Figure S2. Examples of severe colonic pathology in infant rabbits inoculated with *S. flexneri***
698 **infection.**

699 A-B. Haematoxylin and eosin-stained colonic sections of severe hemorrhage in lamina propria
700 and colonic lumen from animals infected with the WT strain at 36 hpi. Arrowheads in (A)
701 indicate either an area of hemorrhage in the lamina propria or hemorrhage spreading to the

lumen (inset, A). (B) Hemorrhage and epithelial cell sloughing in colonic lumen. Scale bar is 100 µm.

Figure S3. Range of IL-8 expression in colons of infected infant rabbits.

(Top left, plot) Percentage of IL-8 expressing cells in each field of view from colonic tissue sections stained with probe to rabbit IL-8 from individual rabbits infected with the WT strain or from uninfected rabbits. Colored dots correspond to micrographs with similar colored borders. Mean values are indicated with bars.

(Micrographs) Immunofluorescence micrographs of colonic sections from uninfected animals or infant rabbits infected with WT *S. flexneri* strain. Sections were stained with a RNAscope probe to rabbit IL-8 (red), and an antibody to *Shigella* (green), and with DAPI (blue).

Figure S4. Localization of *S. flexneri* mutants in infected infant rabbits.

A-C. Immunofluorescence micrographs of *S. flexneri* mutants in colonic tissue of infected rabbits 36 hpi. (A) Inset and white arrows show individual *S. flexneri* Δ*icsA* closely associated with the colonic epithelium. Blue, DAPI; green, FITC-conjugated anti-*Shigella* antibody; red, phalloidin-Alexa 568. Scale bar is 500 µm (A-C).

720 **Supplemental Tables**

721

722 **Table S1. Transposon library in *Shigella flexneri* 2a strain 2457T**

723

724 **Table S2. Strains, plasmids, and oligos**

725

726

References

1. **Legros D, Pierce N**. 2005. Guidelines for the control of shigellosis, including epidemics due to Shigella dysenteriae type 1World Health Organization.

2. **Khalil IA, Troeger C, Blacker BF, Rao PC, Brown A, Atherly DE, Brewer TG, Engmann CM, Houpt ER, Kang G, Kotloff KL, Levine MM, Luby SP, MacLennan CA, Pan WK, Pavlinac PB, Platts-Mills JA, Qadri F, Riddle MS, Ryan ET, Shoultz DA, Steele AD, Walson JL, Sanders JW, Mokdad AH, Murray CJL, Hay SI, Reiner RC**. 2018. Morbidity and mortality due to shigella and enterotoxigenic Escherichia coli diarrhoea: the Global Burden of Disease Study 1990–2016. *Lancet Infect Dis* **18**:1229–1240.

3. **Troeger C, Blacker BF, Khalil IA, Rao PC, Cao S, Zimsen SR, Albertson SB, Stanaway JD, Deshpande A, Abebe Z, Alvis-Guzman N, Amare AT, Asgedom SW, Anteneh ZA, Antonio CAT, Aremu O, Asfaw ET, Atey TM, Atique S, Avokpaho EFGA, Awasthi A, Ayele HT, Barac A, Barreto ML, Bassat Q, Belay SA, Bensenor IM, Bhutta ZA, Bijani A, Bizuneh H, Castañeda-Orjuela CA, Dadi AF, Dandona L, Dandona R, Do HP, Dubey M, Dubljanin E, Edessa D, Endries AY, Eshrati B, Farag T, Feyissa GT, Foreman KJ, Forouzanfar MH, Fullman N, Gething PW, Gishu MD, Godwin WW, Gugnani HC, Gupta R, Hailu GB, Hassen HY, Hibstu DT, Ilesanmi OS, Jonas JB, Kahsay A, Kang G, Kasaeian A, Khader YS, Khan EA, Khan MA, Khang YH, Kissoon N, Kochhar S, Kotloff KL, Koyanagi A, Kumar GA, Magdy Abd El Razek H, Malekzadeh R, Malta DC, Mehata S, Mendoza W, Mengistu DT, Menota BG, Mezgebe HB, Mlashu FW, Murthy S, Naik GA, Nguyen CT, Nguyen TH, Ningrum DNA, Ogbo FA, Olagunju AT, Paudel D, Platts-Mills JA, Qorbani M, Rafay A, Rai RK, Rana SM, Ranabhat CL, Rasella D, Ray SE, Reis C, Renzaho AM, Rezai MS, Ruhago GM, Safiri S, Salomon JA, Sanabria JR, Sartorius B, Sawhney M, Sepanlou SG, Shigematsu M, Sisay M, Somayaji R, Sreeramareddy CT, Sykes BL, Taffere GR, Topor-Madry R, Tran BX, Tuem KB, Ukwaja KN, Vollset SE, Walson JL, Weaver MR, Weldegwergs KG, Werdecker A, Workicho A, Yenesew M, Yirsaw BD, Yonemoto N, El Sayed Zaki M, Vos T, Lim SS, Naghavi M, Murray CJ, Mokdad AH, Hay SI, Reiner RC**. 2018. Estimates of the global, regional, and national morbidity, mortality, and aetiologies of diarrhoea in 195 countries: a systematic analysis for the Global Burden of Disease Study 2016. *Lancet Infect Dis* **18**:1211–1228.

4. **Kotloff KL, Winickoff JP, Ivanoff B, Clemens JD, Swerdlow DL, Sansonetti PJ, Adak GK, Levine MM**. 1999. Global burden of Shigella infections: Implications for vaccine development and implementation of control strategies. *Bull World Health Organ* **77**:651–666.

5. **Ram PK, Crump JA, Gupta SK, Miller MA, Mintz ED**. 2008. Part II. Analysis of data gaps pertaining to Shigella infections in low and medium human development index countries, 1984-2005. *Epidemiol Infect* **136**:577–603.

6. **Livio S, Strockbine NA, Panchalingam S, Tennant SM, Barry EM, Marohn ME, Antonio M, Hossain A, Mandomando I, Ochieng JB, Oundo JO, Qureshi S, Ramamurthy T, Tamboura B, Adegbola RA, Hossain MJ, Saha D, Sen S, Faruque ASG, Alonso PL, Breiman RF, Zaidi AKM, Sur D, Sow SO, Berkeley LY, O'Reilly CE, Mintz ED, Biswas K,**

Cohen D, Farag TH, Nasrin D, Wu Y, Blackwelder WC, Kotloff KL, Nataro JP, Levine MM. 2014. Shigella isolates from the global enteric multicenter study inform vaccine development. *Clin Infect Dis* **59**:933–941.

7. **Thompson CN, Duy PT, Baker S**. 2015. The rising dominance of Shigella sonnei: An intercontinental shift in the etiology of bacillary dysentery. *PLoS Negl Trop Dis* **9**:1–13.

8. **Anand BS, Malhotra V, Bhattacharya SK, Datta P, Datta D, Sen D, Bhattacharya MK, Mukherjee PP, Pal SC**. 1986. Rectal histology in acute bacillary dysentery. *Gastroenterology* **90**:654–60.

9. **Mathan MM, Mathan VI**. 1991. Morphology of rectal mucosa of patients with shigellosis. *Rev Infect Dis* **13 Suppl 4**:S314-8.

10. **Yum LK, Byndloss MX, Feldman SH, Agaisse H**. 2019. Critical role of bacterial dissemination in an infant rabbit model of bacillary dysentery. *Nat Commun* **10**:1–10.

11. **Schroeder GN, Hilbi H**. 2008. Molecular pathogenesis of Shigella spp.: controlling host cell signaling, invasion, and death by type III secretion. *Clin Microbiol Rev* **21**:134–56.

12. **Sansonetti PJ, Kopecko DJ, Formal SB**. 1981. Shigella sonnei plasmids: evidence that a large plasmid is necessary for virulence. *Infect Immun* **34**:75–83.

13. **Sansonetti PJ, Kopecko DJ, Formal SB**. 1982. Involvement of a plasmid in the invasive ability of Shigella flexneri. *Infect Immun* **35**:852–60.

14. **Venkatesan MM, Goldberg MB, Rose DJ, Grotbeck EJ, Burland V, Blattner FR**. 2001. Complete DNA sequence and analysis of the large virulence plasmid of Shigella flexneri. *Infect Immun* **69**:3271–85.

15. **Sasakawa C, Kamata K, Sakai T, Makino S, Yamada M, Okada N, Yoshikawa M**. 1988. Virulence-associated genetic regions comprising 31 kilobases of the 230-kilobase plasmid in Shigella flexneri 2a. *J Bacteriol* **170**:2480–4.

16. **Makino S, Sasakawa C, Kamata K, Kurata T, Yoshikawa M**. 1986. A genetic determinant required for continuous reinfection of adjacent cells on large plasmid in S. flexneri 2a. *Cell* **46**:551–5.

17. **Goldberg MB, Theriot JA**. 1995. Shigella flexneri surface protein IcsA is sufficient to direct actin-based motility. *Proc Natl Acad Sci U S A* **92**:6572–6.

18. **Lederer I, Much P, Allerberger F, Voracek T, Vielgrader H**. 2005. Outbreak of shigellosis in the Vienna Zoo affecting human and non-human primates [3]. *Int J Infect Dis* **9**:290–291.

19. **Formal SB, Gemski P, Baron LS, Labrec EH**. 1971. A Chromosomal Locus Which Controls the Ability of Shigella flexneri to Evoke Keratoconjunctivitis. *Infect Immun* **3**:73–9.

20. **West NP, Sansonetti P, Mounier J, Exley RM, Parsot C, Guadagnini S, Prévost MC, Prochnicka-Chalufour A, Delepierre M, Tanguy M, Tang CM**. 2005. Optimization of virulence functions through glucosylation of Shigella LPS. *Science (80-)* **307**:1313–1317.

21. **Shim D-H, Suzuki T, Chang S-Y, Park S-M, Sansonetti PJ, Sasakawa C, Kweon M-N**. 2007.

New Animal Model of Shigellosis in the Guinea Pig: Its Usefulness for Protective Efficacy Studies. *J Immunol* **178**:2476–2482.

22. **Arena ET, Campbell-Valois FX, Tinevez JY, Nigro G, Sachse M, Moya-Nilges M, Nothelfer K, Marteyn B, Shorte SL, Sansonetti PJ**. 2015. Bioimage analysis of Shigella infection reveals targeting of colonic crypts. *Proc Natl Acad Sci U S A* **112**:E3282–E3290.

23. **Xu D, Liao C, Zhang B, Tolbert WD, He W, Dai Z, Zhang W, Yuan W, Pazgier M, Liu J, Yu J, Sansonetti PJ, Bevins CL, Shao Y, Lu W**. 2018. Human Enteric α-Defensin 5 Promotes Shigella Infection by Enhancing Bacterial Adhesion and Invasion. *Immunity* **48**:1233-1244.e6.

24. **Tinevez J-Y, Arena ET, Anderson M, Nigro G, Injarabian L, André A, Ferrari M, Campbell-Valois F-X, Devin A, Shorte SL, Sansonetti PJ, Marteyn BS**. 2019. Shigella-mediated oxygen depletion is essential for intestinal mucosa colonization. *Nat Microbiol*.

25. **Singer M, Sansonetti PJ**. 2004. IL-8 Is a Key Chemokine Regulating Neutrophil Recruitment in a New Mouse Model of Shigella- Induced Colitis . *J Immunol* **173**:4197–4206.

26. **VOINO-YASENETSKY M V, VOINO-YASENETSKAYA MK**. 1962. Experimental pneumonia caused by bacteria of the Shigella group. *Acta Morphol Acad Sci Hung* **11**:439–54.

27. **Mallett CP, VanDeVerg L, Collins HH, Hale TL**. 1993. Evaluation of Shigella vaccine safety and efficacy in an intranasally challenged mouse model. *Vaccine* **11**:190–196.

28. **Van de Verg LL, Mallett CP, Collins HH, Larsen T, Hammack C, Hale TL**. 1995. Antibody and cytokine responses in a mouse pulmonary model of Shigella flexneri serotype 2a infection. *Infect Immun* **63**:1947–1954.

29. **Way SS, Borczuk AC, Dominitz R, Goldberg MB**. 1998. An Essential Role for Gamma Interferon in Innate Resistance to Shigella flexneri Infection. *Infect Immun* **66**:1342–1348.

30. **Fernandez MI, Thuizat A, Pedron T, Neutra M, Phalipon A, Sansonetti PJ**. 2003. A newborn mouse model for the study of intestinal pathogenesis of shigellosis. *Cell Microbiol* **5**:481–491.

31. **Fernandez M-I, Regnault B, Mulet C, Tanguy M, Jay P, Sansonetti PJ, Pédron T**. 2008. Maturation of Paneth Cells Induces the Refractory State of Newborn Mice to Shigella Infection . *J Immunol* **180**:4924–4930.

32. **Mostowy S, Boucontet L, Mazon Moya MJ, Sirianni A, Boudinot P, Hollinshead M, Cossart P, Herbomel P, Levraud J-P, Colucci-Guyon E**. 2013. The zebrafish as a new model for the in vivo study of Shigella flexneri interaction with phagocytes and bacterial autophagy. *PLoS Pathog* **9**:e1003588.

33. **Duggan GM, Mostowy S**. 2018. Use of zebrafish to study Shigella infection. *Dis Model Mech* **11**:1–11.

34. **Ritchie JM, Thorpe CM, Rogers AB, Waldor MK**. 2003. Critical roles for stx2, eae, and tir in enterohemorrhagic Escherichia coli-induced diarrhea and intestinal inflammation in

844 infant rabbits. *Infect Immun* **71**:7129–39.

845 35. **Ritchie JM, Rui H, Bronson RT, Waldor MK**. 2010. Back to the future: Studying cholera
846 pathogenesis using infant Rabbits. *MBio* **1**:1–13.

847 36. **Ritchie JM, Rui H, Zhou X, Iida T, Kodoma T, Ito S, Davis BM, Bronson RT, Waldor MK**.
848 2012. Inflammation and disintegration of intestinal villi in an experimental model for
849 vibrio parahaemolyticus-induced diarrhea. *PLoS Pathog* **8**.

850 37. **Porter CK, Lynen A, Riddle MS, Talaat K, Sack D, Gutiérrez RL, McKenzie R, DeNearing B,**
851 **Feijoo B, Kaminski RW, Taylor DN, Kirkpatrick BD, Bourgeois AL**. 2018. Clinical endpoints
852 in the controlled human challenge model for Shigella: A call for standardization and the
853 development of a disease severity score. *PLoS One* **13**:e0194325.

854 38. **Gomez HF, Ochoa TJ, Herrera-Insua I, Carlin LG, Cleary TG**. 2002. Lactoferrin protects
855 rabbits from Shigella flexneri-induced inflammatory enteritis. *Infect Immun* **70**:7050–3.

856 39. **Gomez HF, Ochoa TJ, Carlin LG, Cleary TG**. 2003. Human lactoferrin impairs virulence of
857 Shigella flexneri. *J Infect Dis* **187**:87–95.

858 40. **Kadurugamuwa JL, Rohde M, Wehland J, Timmis KN**. 1991. Intercellular spread of
859 Shigella flexneri through a monolayer mediated by membranous protrusions and
860 associated with reorganization of the cytoskeletal protein vinculin. *Infect Immun*
861 **59**:3463–71.

862 41. **Monack DM, Theriot JA**. 2001. Actin-based motility is sufficient for bacterial membrane
863 protrusion formation and host cell uptake. *Cell Microbiol* **3**:633–47.

864 42. **Lecuit M, Vandormael-Pournin S, Lefort J, Huerre M, Gounon P, Dupuy C, Babinet C,**
865 **Cossart P**. 2001. A transgenic model for listeriosis: Role of internalin in crossing the
866 intestinal barrier. *Science (80-)* **292**:1722–1725.

867 43. **Zhang T, Abel S, Abel Zur Wiesch P, Sasabe J, Davis BM, Higgins DE, Waldor MK**. 2017.
868 Deciphering the landscape of host barriers to Listeria monocytogenes infection. *Proc Natl*
869 *Acad Sci U S A* **114**:6334–6339.

870 44. **Maury MM, Bracq-Dieye H, Huang L, Vales G, Lavina M, Thouvenot P, Disson O,**
871 **Leclercq A, Brisse S, Lecuit M**. 2019. Hypervirulent Listeria monocytogenes clones'
872 adaption to mammalian gut accounts for their association with dairy products. *Nat*
873 *Commun* **10**:2488.

874 45. **Lawley TD, Bouley DM, Hoy YE, Gerke C, Relman DA, Monack DM**. 2008. Host
875 transmission of Salmonella enterica serovar Typhimurium is controlled by virulence
876 factors and indigenous intestinal microbiota. *Infect Immun* **76**:403–16.

877 46. **Suwandi A, Galeev A, Riedel R, Sharma S, Seeger K, Sterzenbach T, García Pastor L,**
878 **Boyle EC, Gal-Mor O, Hensel M, Casadesús J, Baines JF, Grassl GA**. 2019. Std fimbriae-
879 fucose interaction increases Salmonella-induced intestinal inflammation and prolongs
880 colonization. *PLoS Pathog* **15**:e1007915.

881 47. **Waugh DJJ, Wilson C**. 2008. The interleukin-8 pathway in cancer. *Clin Cancer Res*

14:6735–41.

48. **Schnupf P, Sansonetti PJ**. 2012. Quantitative RT-PCR profiling of the rabbit immune response: assessment of acute Shigella flexneri infection. *PLoS One* **7**:e36446.

49. **Raqib R, Lindberg AA, Wretlind B, Bardhan PK, Andersson U, Andersson J**. 1995. Persistence of local cytokine production in shigellosis in acute and convalescent stages. *Infect Immun* **63**:289–296.

50. **Raqib R, Wretlind B, Andersson J, Lindberg AA**. 1995. Cytokine secretion in acute shigellosis is correlated to disease activity and directed more to stool than to plasma. *J Infect Dis* **171**:376–84.

51. **Puhar A, Tronchère H, Payrastre B, Tran Van Nhieu G, Sansonetti PJ**. 2013. A Shigella Effector Dampens Inflammation by Regulating Epithelial Release of Danger Signal ATP through Production of the Lipid Mediator PtdIns5P. *Immunity* **39**:1121–1131.

52. **Arbibe L, Kim DW, Batsche E, Pedron T, Mateescu B, Muchardt C, Parsot C, Sansonetti PJ**. 2007. An injected bacterial effector targets chromatin access for transcription factor NF-κB to alter transcription of host genes involved in immune responses. *Nat Immunol* **8**:47–56.

53. **Pritchard JR, Chao MC, Abel S, Davis BM, Baranowski C, Zhang YJ, Rubin EJ, Waldor MK**. 2014. ARTIST: High-Resolution Genome-Wide Assessment of Fitness Using Transposon-Insertion Sequencing. *PLoS Genet* **10**.

54. **Hubbard TP, Billings G, Dörr T, Sit B, Warr AR, Kuehl CJ, Kim M, Delgado F, Mekalanos JJ, Lewnard JA, Waldor MK**. 2018. A live vaccine rapidly protects against cholera in an infant rabbit model. *Sci Transl Med* **10**:1–11.

55. **Hubbard TP, Chao MC, Abel S, Blondel CJ, Abel zur Wiesch P, Zhou X, Davis BM, Waldor MK**. 2016. Genetic analysis of *Vibrio parahaemolyticus* intestinal colonization. *Proc Natl Acad Sci* **113**:6283–6288.

56. **Warr AR, Hubbard TP, Munera D, Blondel CJ, Abel Zur Wiesch P, Abel S, Wang X, Davis BM, Waldor MK**. 2019. Transposon-insertion sequencing screens unveil requirements for EHEC growth and intestinal colonization. *PLoS Pathog* **15**:e1007652.

57. **Schuch R, Maurelli AT**. 1999. The Mxi-Spa type III secretory pathway of Shigella flexneri requires an outer membrane lipoprotein, MxiM, for invasin translocation. *Infect Immun* **67**:1982–1991.

58. **Schuch R, Maurelli AT**. 2001. MxiM and MxiJ, base elements of the Mxi-Spa type III secretion system of Shigella, interact with and stabilize the MxiD secretin in the cell envelope. *J Bacteriol* **183**:6991–6998.

59. **Burkinshaw BJ, Strynadka NCJ**. 2014. Assembly and structure of the T3SS. *Biochim Biophys Acta - Mol Cell Res* **1843**:1649–1663.

60. **Buffie CG, Bucci V, Stein RR, McKenney PT, Ling L, Gobourne A, No D, Liu H, Kinnebrew M, Viale A, Littmann E, van den Brink MRM, Jenq RR, Taur Y, Sander C, Cross JR,**

Toussaint NC, Xavier JB, Pamer EG. 2015. Precision microbiome reconstitution restores bile acid mediated resistance to Clostridium difficile. *Nature* **517**:205–8.

61. **Becattini S, Littmann ER, Carter RA, Kim SG, Morjaria SM, Ling L, Gyaltshen Y, Fontana E, Taur Y, Leiner IM, Pamer EG**. 2017. Commensal microbes provide first line defense against Listeria monocytogenes infection. *J Exp Med* **214**:1973–1989.

62. **Zhao W, Caro F, Robins W, Mekalanos JJ**. 2018. Antagonism toward the intestinal microbiota and its effect on Vibrio cholerae virulence. *Science (80-)* **359**:210–213.

63. **Formal SB, Kent TH, May HC, Palmer A, Falkow S, LaBrec EH**. 1966. Protection of monkeys against experimental shigellosis with a living attenuated oral polyvalent dysentery vaccine. *J Bacteriol* **92**:17–22.

64. **Formal SB, Oaks E V., Olsen RE, Wingfield-Eggleston M, Snoy PJ, Cogan JP**. 1991. Effect of prior infection with virulent shigella flexneri 2a on the resistance of monkeys to subsequent infection with shigella sonnei. *J Infect Dis* **164**:533–537.

65. **Coster TS, Hoge CW, VanDeVerg LL, Hartman AB, Oaks E V., Venkatesan MM, Cohen D, Robin G, Fontaine-Thompson A, Sansonetti PJ, Hale TL**. 1999. Vaccination against shigellosis with attenuated Shigella flexneri 2a strain SC602. *Infect Immun* **67**:3437–43.

66. **Porter CK, Thura N, Ranallo RT, Riddle MS**. 2013. The Shigella human challenge model. *Epidemiol Infect* **141**:223–232.

67. **Ritchie JM, Thorpe CM, Rogers AB, Waldor MK**. 2003. Critical roles for stx2, eae, and tir in enterohemorrhagic Escherichia coli-induced diarrhea and intestinal inflammation in infant rabbits. *Infect Immun* **71**:7129–39.

68. **Brotcke Zumsteg A, Goosmann C, Brinkmann V, Morona R, Zychlinsky A**. 2014. IcsA is a Shigella flexneri adhesion regulated by the type III secretion system and required for pathogenesis. *Cell Host Microbe* **15**:435–445.

69. **Abel S, Abel zur Wiesch P, Davis BM, Waldor MK**. 2015. Analysis of Bottlenecks in Experimental Models of Infection. *PLoS Pathog* **11**:e1004823.

70. **Wei L, Qiao H, Sit B, Yin K, Yang G, Ma R, Ma J, Yang C, Yao J, Ma Y, Xiao J, Liu X, Zhang Y, Waldor MK, Wang Q**. 2019. A Bacterial Pathogen Senses Host Mannose to Coordinate Virulence. *iScience* **20**:310–323.

71. **Barthel M, Hapfelmeier S, Quintanilla-Martínez L, Kremer M, Rohde M, Hogardt M, Pfeffer K, Rüssmann H, Hardt W-D**. 2003. Pretreatment of mice with streptomycin provides a Salmonella enterica serovar Typhimurium colitis model that allows analysis of both pathogen and host. *Infect Immun* **71**:2839–58.

72. **Becattini S, Littmann ER, Carter RA, Kim SG, Morjaria SM, Ling L, Gyaltshen Y, Fontana E, Taur Y, Leiner IM, Pamer EG**. 2017. Commensal microbes provide first line defense against Listeria monocytogenes infection. *J Exp Med* **214**:1973–1989.

73. **Holt KE, Baker S, Weill FX, Holmes EC, Kitchen A, Yu J, Sangal V, Brown DJ, Coia JE, Kim DW, Choi SY, Kim SH, Da Silveira WD, Pickard DJ, Farrar JJ, Parkhill J, Dougan G,**

Thomson NR. 2012. Shigella sonnei genome sequencing and phylogenetic analysis indicate recent global dissemination from Europe. *Nat Genet* **44**:1056–1059.

74. **Connor TR, Barker CR, Baker KS, Weill FX, Talukder KA, Smith AM, Baker S, Gouali M, Thanh DP, Azmi IJ, da Silveira WD, Semmler T, Wieler LH, Jenkins C, Cravioto A, Faruque SM, Parkhill J, Kim DW, Keddy KH, Thomson NR**. 2015. Species-wide whole genome sequencing reveals historical global spread and recent local persistence in Shigella flexneri. *Elife* **4**:1–16.

75. **Puzari M, Sharma M, Chetia P**. 2018. Emergence of antibiotic resistant Shigella species: A matter of concern. *J Infect Public Health* **11**:451–454.

76. **Abbasi E, Abtahi H, van Belkum A, Ghaznavi-Rad E**. 2019. Multidrug-resistant Shigella infection in pediatric patients with diarrhea from central Iran. *Infect Drug Resist* **12**:1535–1544.

77. **Datsenko KA, Wanner BL**. 2000. One-step inactivation of chromosomal genes in Escherichia coli K-12 using PCR products. *Proc Natl Acad Sci U S A* **97**:6640–5.

78. **Abel S, Waldor MK**. 2015. Infant Rabbit Model for Diarrheal Diseases. *Curr Protoc Microbiol* **38**:6A.6.1-15.

79. **Chiang SL, Rubin EJ**. 2002. Construction of a mariner-based transposon for epitope-tagging and genomic targeting. *Gene* **296**:179–85.

80. **Chao MC, Pritchard JR, Zhang YJ, Rubin EJ, Livny J, Davis BM, Waldor MK**. 2013. High-resolution definition of the Vibrio cholerae essential gene set with hidden Markov model-based analyses of transposon-insertion sequencing data. *Nucleic Acids Res* **41**:9033–9048.

81. **Ferrières L, Hémery G, Nham T, Guérout A-M, Mazel D, Beloin C, Ghigo J-M**. 2010. Silent mischief: bacteriophage Mu insertions contaminate products of Escherichia coli random mutagenesis performed using suicidal transposon delivery plasmids mobilized by broad-host-range RP4 conjugative machinery. *J Bacteriol* **192**:6418–27.

82. **Kimura S, Waldor MK**. 2019. The RNA degradosome promotes tRNA quality control through clearance of hypomodified tRNA. *Proc Natl Acad Sci* **116**:1394–1403.

Figure 1

A

Strain	WT	uninfected	Δ*icsA*	Δ*mxiM*	Plasmid -
Diarrhea	13/22 (59%)	0/8 (0%)	0/10 (0%)	0/12 (0%)	0/12 (0%)
Death	6/22 (27%)	0/8 (0%)	0/10 (0%)	0/12 (0%)	0/12 (0%)
P-value for diarrhea (vs. WT)	-	4.40E-03	1.60E-03	6.00E-04	6.00E-04

B

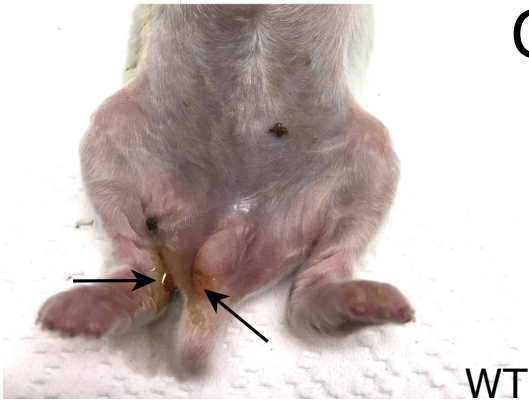

C

D

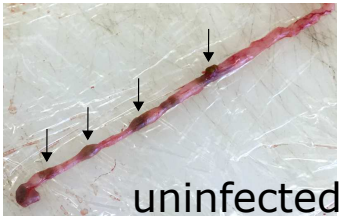

E

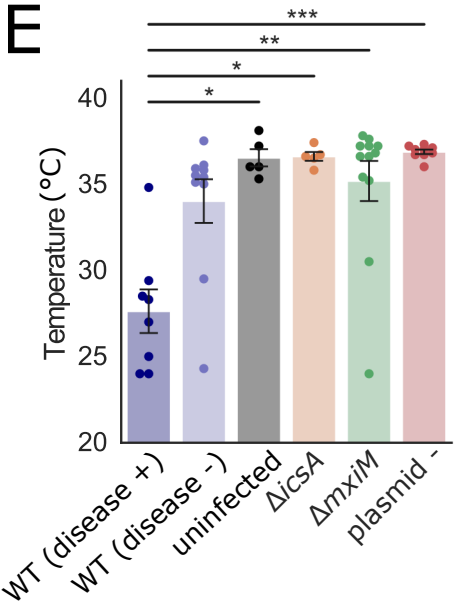

F

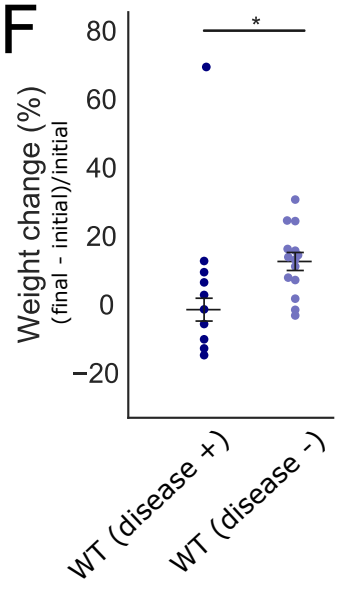

Figure 2

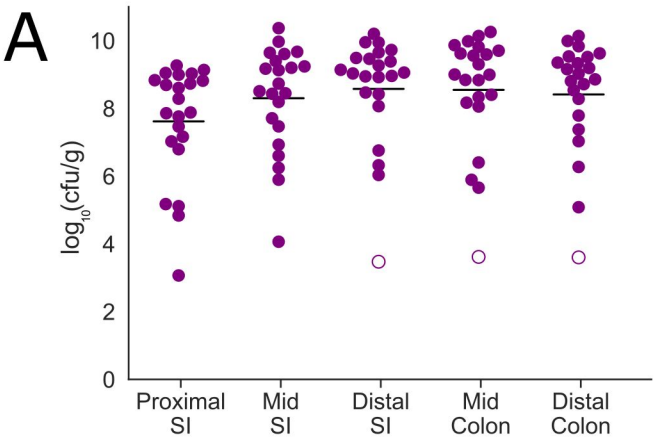
A
10
8
6
4
2
0
log10(cfu/g)
Proximal SI
Mid SI
Distal SI
Mid Colon
Distal Colon

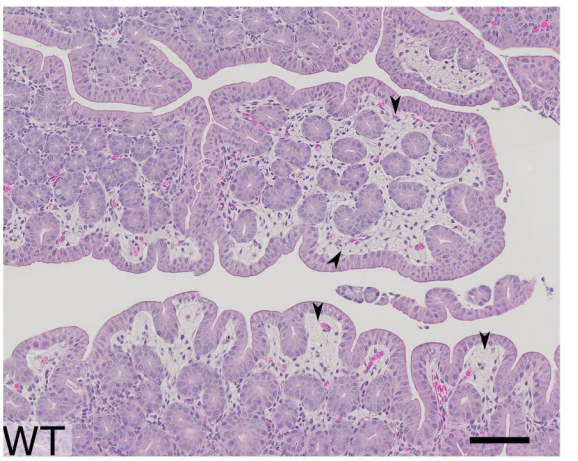
B
WT

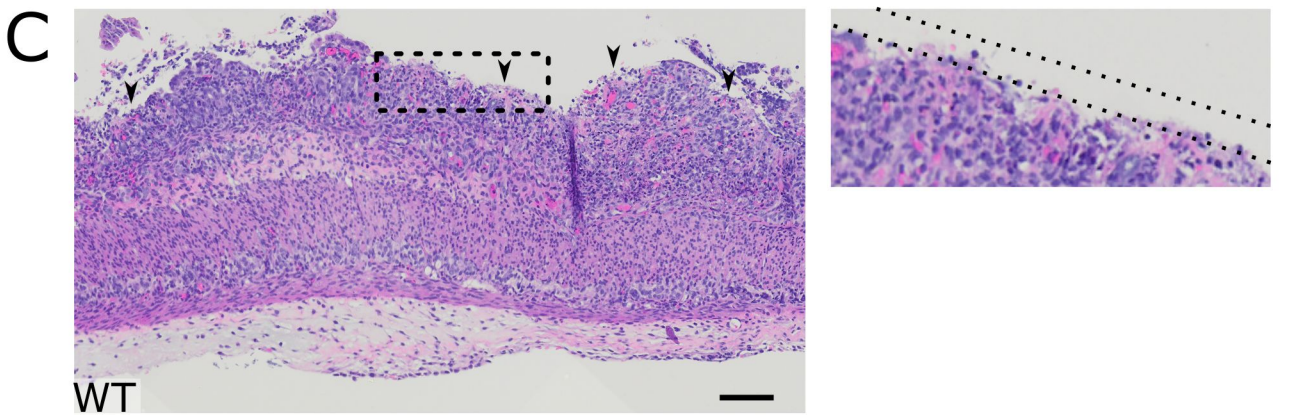
C
WT

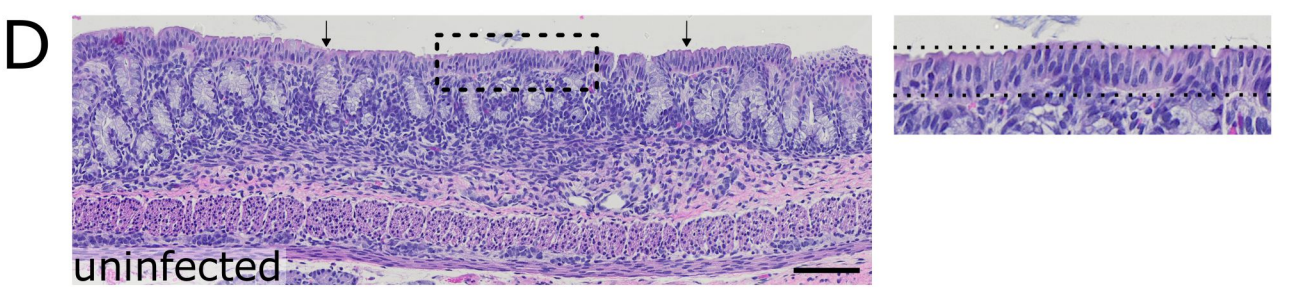
D
uninfected

Figure 3

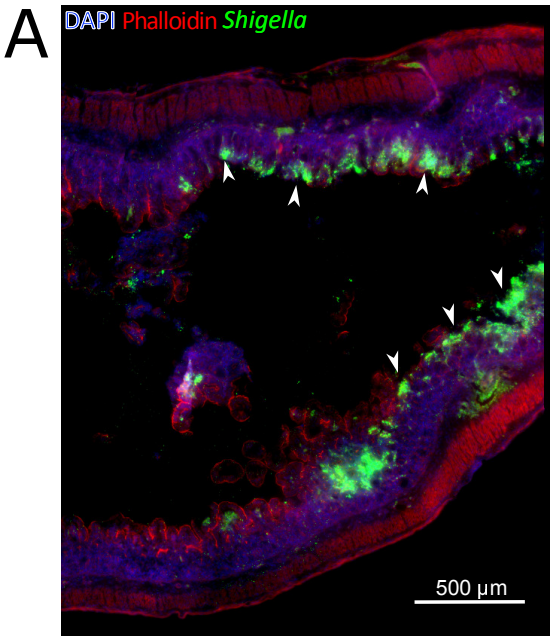
A
DAPI Phalloidin Shigella
500 µm

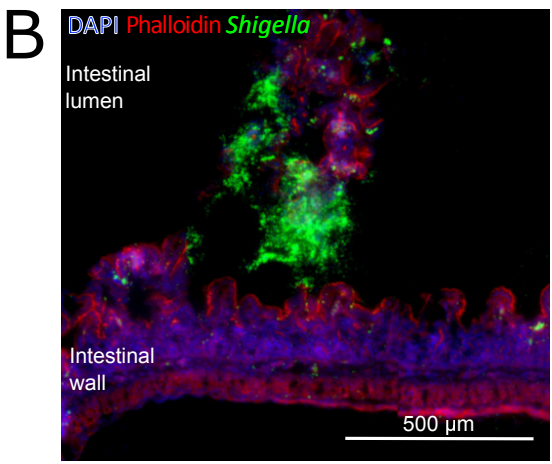
B
DAPI Phalloidin Shigella
Intestinal lumen
Intestinal wall
500 µm

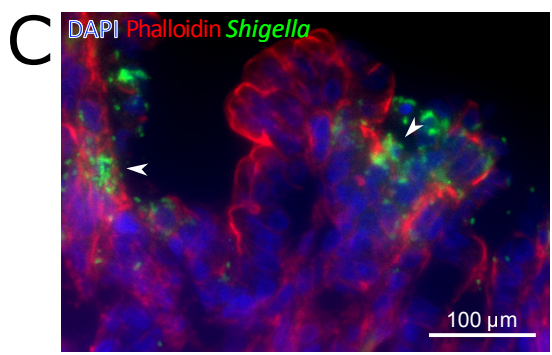
C
DAPI Phalloidin Shigella
100 µm

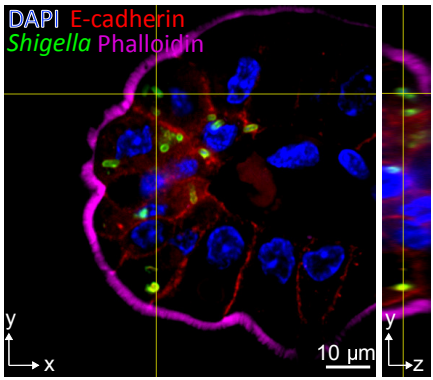
D
DAPI E-cadherin
Shigella Phalloidin
y
x
10 µm
y
z

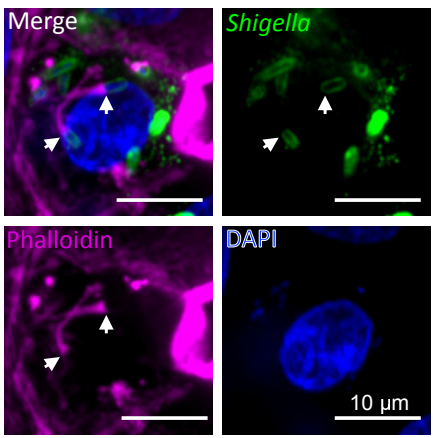
E
Merge
Shigella
Phalloidin
DAPI
10 µm

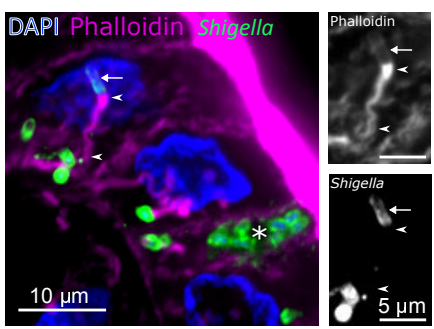
F
DAPI Phalloidin Shigella
10 µm
Phalloidin
Shigella
5 µm

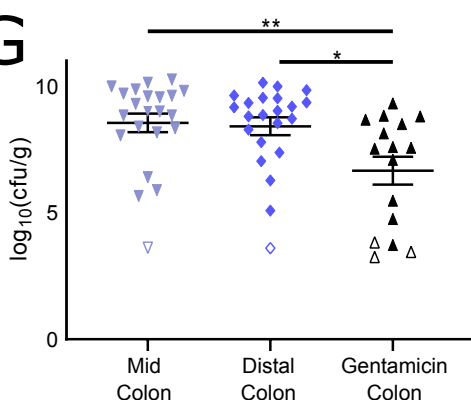
G
**
*
10
5
0
log10(cfu/g)
Mid Colon
Distal Colon
Gentamicin Colon

Figure 4

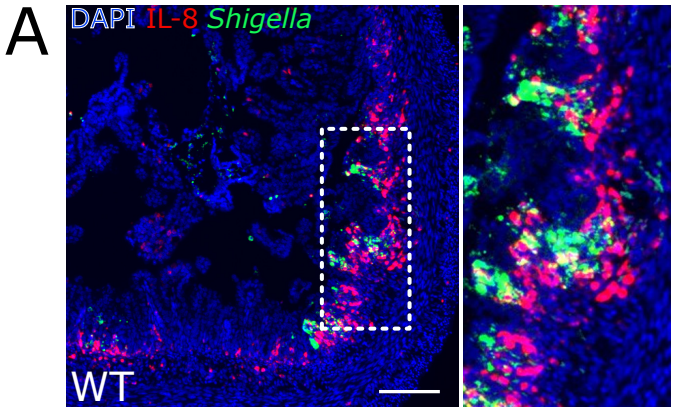
A
DAPI IL-8 Shigella
WT

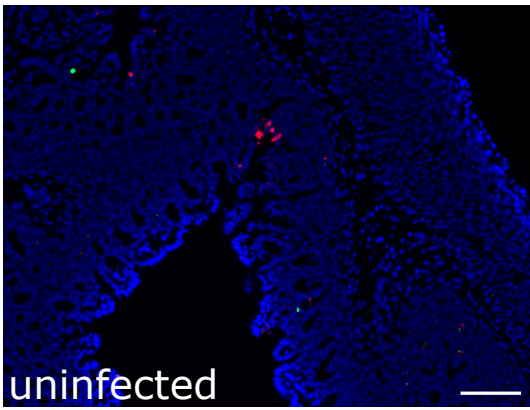
C
uninfected

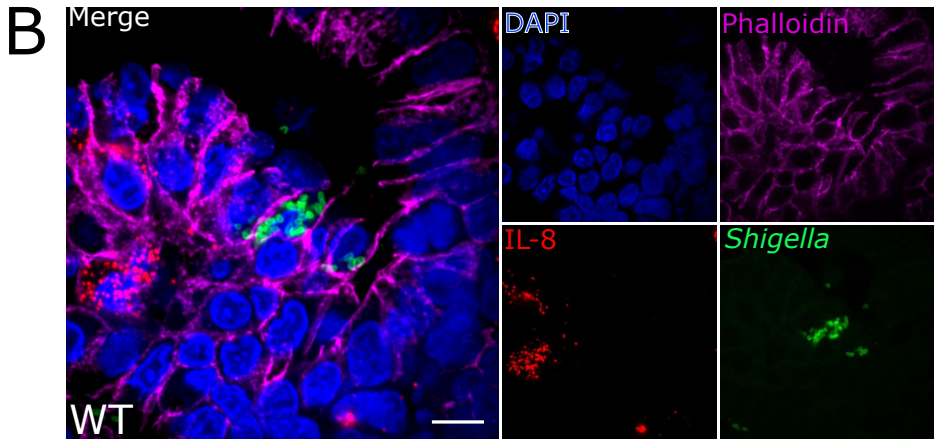
B
Merge
DAPI
Phalloidin
IL-8
Shigella
WT

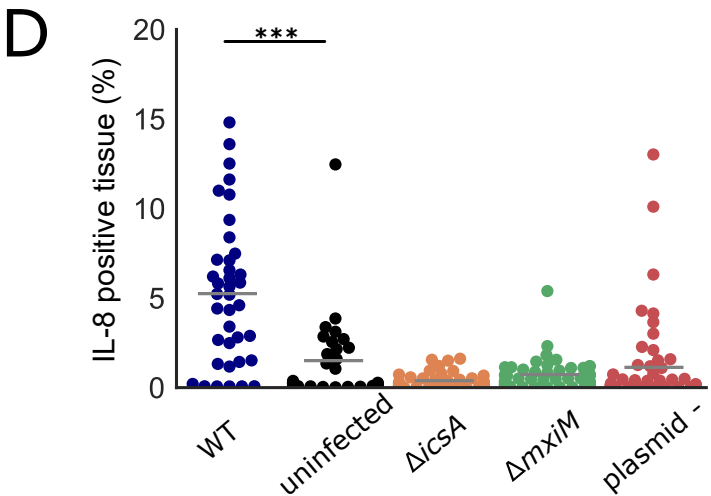
D
IL-8 positive tissue (%)
20
15
10
5
0
***
WT
uninfected
ΔicsA
ΔmxiM
plasmid -

Figure 5

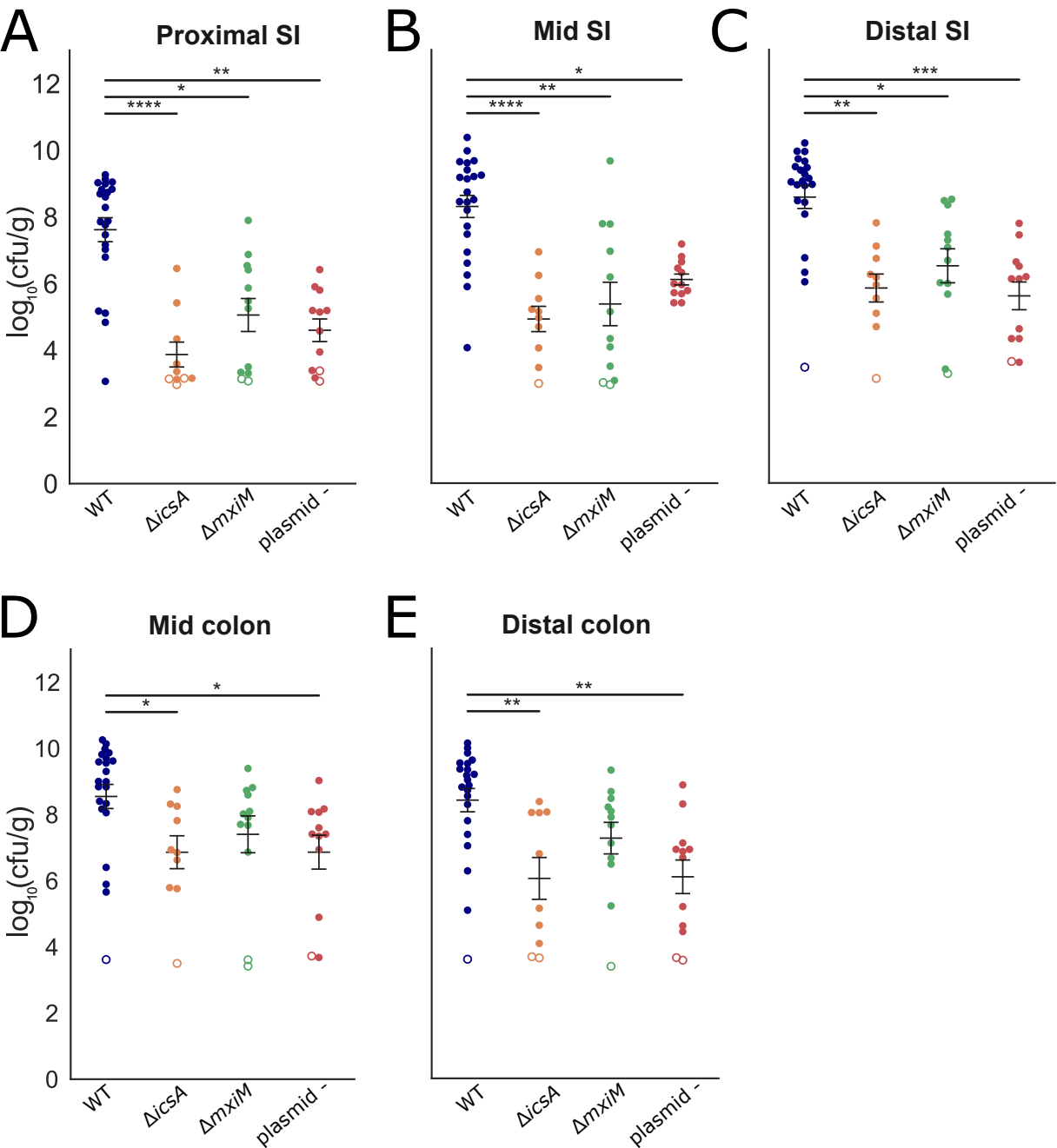
A
Proximal SI
B
Mid SI
C
Distal SI
D
Mid colon
E
Distal colon
log10(cfu/g)
WT
ΔicsA
ΔmxiM
plasmid -

Figure 6

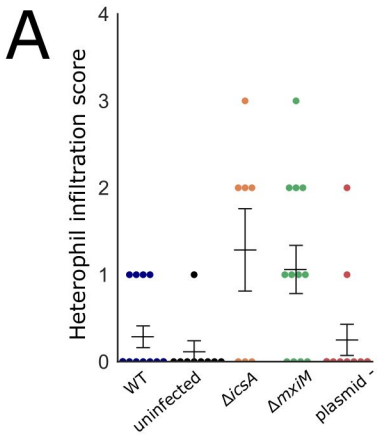
A
Heterophil infiltration score
4
3
2
1
0
WT
uninfected
ΔicsA
ΔmxiM
plasmid -

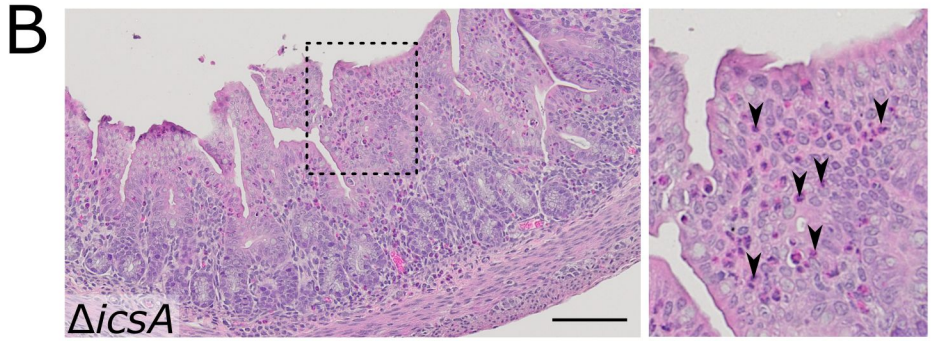
B
ΔicsA

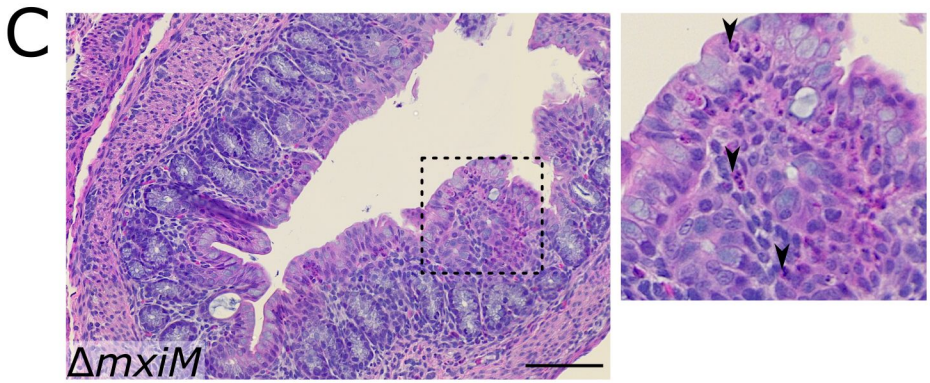
C
ΔmxiM

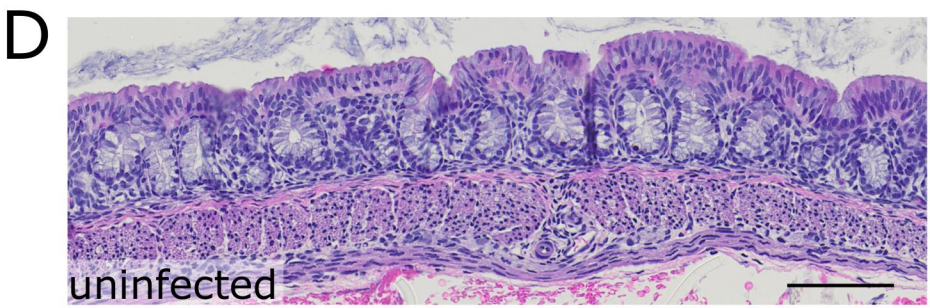
D
uninfected

Figure 7

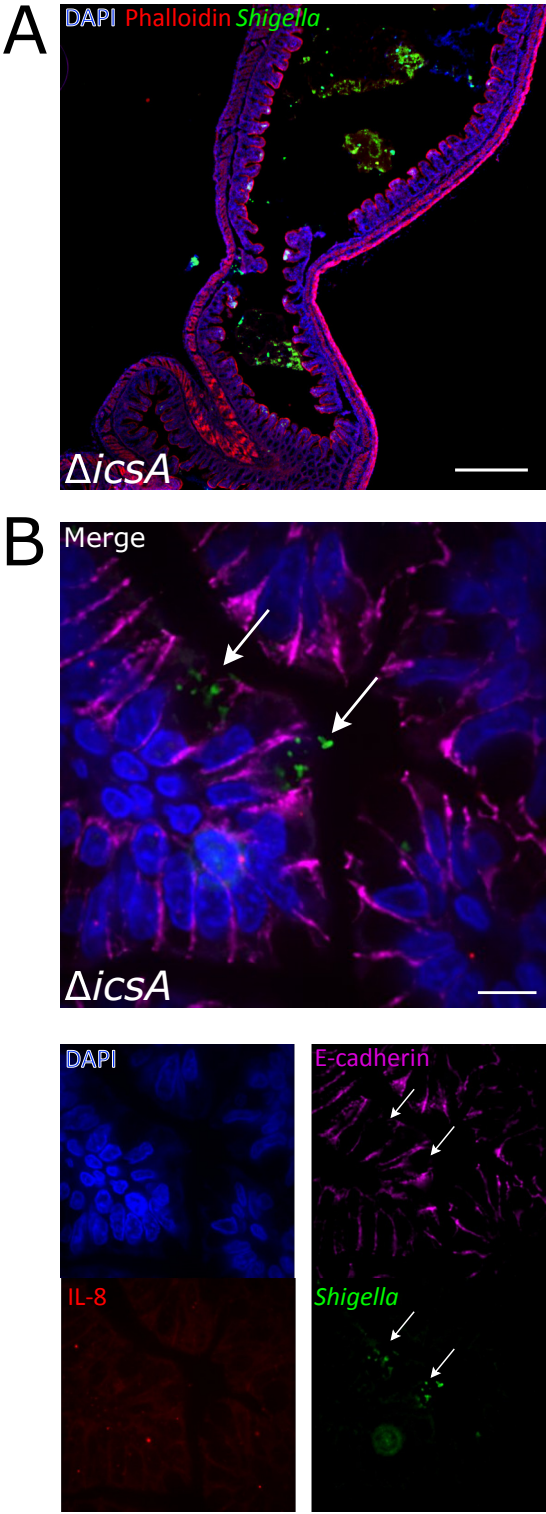
A
DAPI Phalloidin Shigella
ΔicsA
B
Merge
ΔicsA
DAPI
E-cadherin
IL-8
Shigella